

Revisiting $B \rightarrow \pi K, \pi K^*$ and ρK Decays: CP Violations and Implication for New Physics

Qin Chang^{a,b}, Xin-Qiang Li^{c*}, Ya-Dong Yang^{a†}

^aInstitute of Particle Physics, Huazhong Normal University, Wuhan, Hubei 430079, P. R. China

^bDepartment of Physics, Henan Normal University, Xinxiang, Henan 453007, P. R. China

^cInstitut für Theoretische Physik E, RWTH Aachen, D-52056, Aachen, Germany

Abstract

Combining the up-to-date experimental information on $B \rightarrow \pi K, \pi K^*$ and ρK decays, we revisit the decay rates and CP asymmetries of these decays within the framework of QCD factorization. Using an infrared finite gluon propagator of Cornwall prescription, we find that the time-like annihilation amplitude could contribute a large strong phase, while the space-like hard spectator scattering amplitude is real. Numerically, we find that all the branching ratios and most of the direct CP violations, except $A_{CP}(B^\pm \rightarrow K^\pm \pi^0)$, agree with the current experimental data with an effective gluon mass $m_g \simeq 0.5$ GeV. Taking the unmatched difference in direct CP violations between $B \rightarrow \pi^0 K^\pm$ and $\pi^\mp K^\pm$ decays as a hint of new physics, we perform a model-independent analysis of new physics contributions with a set of $\bar{s}(1 + \gamma_5)b \otimes \bar{q}(1 + \gamma_5)q$ ($q=u,d$) operators. Detail analyses of the relative impacts of the operators are presented in five cases. Fitting the twelve decay modes, parameter spaces are found generally with nontrivial weak phases. Our results may indicate that both strong phase from annihilation amplitude and new weak phase from new physics are needed to resolve the πK puzzle. To further test the new physics hypothesis, the mixing-induced CP violations in $B \rightarrow \pi^0 K_S$ and $\rho^0 K_S$ are discussed and good agreements with the recent experimental data are found.

*Alexander-von-Humboldt Fellow

†Corresponding author

1 Introduction

With the fruitful running of BABAR and Belle in past decade, plenty of exciting results has been produced, which provides a very fertile testing ground for the Standard Model (SM) picture of flavor physics and CP violations. Although most of the measurements are in perfect agreement with the SM predictions, there still exist some unexplained mismatches. Especially, a combination of experimental data on a set of related decays will increase the tension between the SM predictions and experimental measurements. At present, there are discrepancies between the measurement of several observables in $B \rightarrow \pi K$ decays and the predications of the SM, the so-called “ πK puzzle” [1], which have attracted extensive investigations in the SM [2, 3, 4, 5, 6, 7], as well as with various specific New Physics (NP) scenarios [8].

Recently, Belle has measured the direct CP violations $B \rightarrow K\pi$ decays [9]

$$A_{CP}(B^- \rightarrow K^- \pi^0) \equiv \frac{\Gamma(B^- \rightarrow K^- \pi^0) - \Gamma(B^+ \rightarrow K^+ \pi^0)}{\Gamma(B^- \rightarrow K^- \pi^0) + \Gamma(B^+ \rightarrow K^+ \pi^0)} = +0.07 \pm 0.03 \pm 0.01, \quad (1)$$

$$A_{CP}(\bar{B}^0 \rightarrow K^- \pi^+) \equiv \frac{\Gamma(\bar{B}^0 \rightarrow K^- \pi^+) - \Gamma(B^0 \rightarrow K^+ \pi^-)}{\Gamma(\bar{B}^0 \rightarrow K^- \pi^+) + \Gamma(B^0 \rightarrow K^+ \pi^-)} = -0.094 \pm 0.018 \pm 0.008. \quad (2)$$

The difference between direct CP violations in charged and neutral modes is

$$\Delta A \equiv A_{CP}(B^- \rightarrow K^- \pi^0) - A_{CP}(\bar{B}^0 \rightarrow K^- \pi^+) = 0.164 \pm 0.037. \quad (3)$$

The averages of the current experimental data of BABAR [10], Belle [9], CLEO [11] and CDF [12] by the Heavy Flavor Averaging Group (HFAG) [13] are

$$\begin{aligned} A_{CP}(B^- \rightarrow K^- \pi^0) &= 0.050 \pm 0.025, \\ A_{CP}(\bar{B}^0 \rightarrow K^- \pi^+) &= -0.097 \pm 0.012, \end{aligned} \quad (4)$$

and the difference $\Delta A = 0.147 \pm 0.028$ is established at 5σ level. However, within the SM, it is generally expected that $A_{CP}(\bar{B}_d^0 \rightarrow \pi^+ K^-)$ and $A_{CP}(B_u^- \rightarrow \pi^0 K^-)$ are close to each other. For example, the recent theoretical predictions for these two quantities based on the QCD factorization approach (QCDF)[14], the perturbative QCD approach (pQCD)[15] and the

soft-collinear effective theory (SCET) [16] read

$$\left\{ \begin{array}{l} A_{CP}(B_u^- \rightarrow \pi^0 K^-)_{QCDF} = -3.6\% , \\ A_{CP}(\bar{B}_d^0 \rightarrow \pi^+ K^-)_{QCDF} = -4.1\% ; \end{array} \right. \quad \text{QCDF Scenario S4 [3]} \quad (5)$$

$$\left\{ \begin{array}{l} A_{CP}(B_u^- \rightarrow \pi^0 K^-)_{pQCD} = (-1_{-5}^{+3})\% , \\ A_{CP}(\bar{B}_d^0 \rightarrow \pi^+ K^-)_{pQCD} = (-9_{-8}^{+6})\% ; \end{array} \right. \quad \text{pQCD [5]} \quad (6)$$

$$\left\{ \begin{array}{l} A_{CP}(B_u^- \rightarrow \pi^0 K^-)_{SCET} = (-11 \pm 9 \pm 11 \pm 2)\% , \\ A_{CP}(\bar{B}_d^0 \rightarrow \pi^+ K^-)_{SCET} = (-6 \pm 5 \pm 6 \pm 2)\% . \end{array} \right. \quad \text{SCET [6]} \quad (7)$$

We can see that the present theoretical estimations within the SM are confronted with the established ΔA . The mismatch may be due to our limited understanding of the strong dynamics in B decays which hinders precise estimations of the SM contributions, but equally possible due to new physics effects [17, 18].

As is known, the annihilation decay of B meson into two light mesons offers interesting probes for the dynamical mechanism governing these decays, as well as the exploration of CP violation. In most of B meson non-leptonic decays, the annihilation corrections could generate some strong phases, which are important for estimating CP violation. However, unlike the vertex-type correction amplitude, the calculation of annihilation amplitude always suffers from end-point divergence in collinear factorization approach. In the pQCD approach, such divergence is regulated by the parton transverse momentum k_T at expense of modeling additional k_T dependence of meson distribution functions [15], and a large strong phase is found. In the QCD factorization (QCDF) approach [14], to give a conservative estimation, the divergence is parameterized by complex parameters, $X_A = \int_0^1 dy/y = \ln(m_b/\Lambda)(1 + \rho_A e^{i\phi_A})$, with $\rho_A \leq 1$ and unrestricted ϕ_A , which will sometimes introduce large theoretical uncertainties in the final results. In Refs. [6, 19], annihilation diagram is studied with SCET and also parameterized by a complex amplitude. At present, the dynamical origin of these corrections still remains a theoretical challenge.

In this paper, we will revisit $B \rightarrow \pi K$, πK^* and ρK decays within QCDF framework. However, we shall quote the infrared finite gluon propagator of Cornwall prescription [20] to regulate these divergences in hard-spectator scattering and annihilation amplitudes. With this alternative scheme, we could evaluate both the strength and the strong phase of hard spectator and annihilation corrections at the expense of a dynamic gluon mass, which will be fitted in the

twelve decay modes. It is interesting to note that the infrared finite behavior of gluon propagator are not only obtained from solving the well known Schwinger-Dyson equation [20, 21, 22], but also supported by recent Lattice QCD simulations [23]. Numerically, a sizable strength and a large strong phase of annihilation corrections are found. Except $A_{CP}(B^\pm \rightarrow K^\pm \pi^0)$, our predictions for most of the branching ratios and the direct CP asymmetries of $B \rightarrow \pi K$, πK^* and ρK agree with the current experimental data with an effective gluon mass $m_g = 0.45 \sim 0.55$ GeV. However, we get $A_{CP}(B^\pm \rightarrow K^\pm \pi^0) = -0.109 \pm 0.008$ which is still in sharp contrast to experimental data 0.050 ± 0.025 . To resolve this mismatch, we perform a model-independent analysis of new physics contributions with a set of flavor-changing neutral current (FCNC) $\bar{s}(1 + \gamma_5)b \otimes \bar{q}(1 + \gamma_5)q$ (q=u,d) operators. To fit the twelve decay modes, parameter spaces are found generally with large weak phases. Our results indicate that both strong phase from annihilation amplitude and new weak phase from new physics are needed to account for the experimental data.

In Section 2, we revisit $B \rightarrow \pi K$, πK^* and ρK decays in the SM with QCDF modified by an infrared finite gluon propagator for annihilation and spectator scattering kernels. After recalculating the hard-spectator scattering and the weak annihilation corrections, we present our numerical results and discussions. In Section 3, to find resolution to the CP violation difference ΔA , we present analyses of NP operators. Then, using the constrained parameters for the operators, we discuss the mixing-induced CP violations in $B \rightarrow \pi^0 K_S$ and $\rho^0 K_S$. Section 4 contains our conclusions. Appendix A recapitulates the decay amplitudes for the twelve decay modes within the SM [3]. All the theoretical input parameters are summarized in Appendix B.

2 Revisiting $B \rightarrow \pi K$, πK^* and ρK Decays in the SM

In the SM, the effective weak Hamiltonian responsible for $b \rightarrow s$ transitions is given as [24]

$$\begin{aligned} \mathcal{H}_{\text{eff}} = & \frac{G_F}{\sqrt{2}} \left[V_{ub}V_{us}^* (C_1 O_1^u + C_2 O_2^u) + V_{cb}V_{cs}^* (C_1 O_1^c + C_2 O_2^c) - V_{tb}V_{ts}^* \left(\sum_{i=3}^{10} C_i O_i \right. \right. \\ & \left. \left. + C_{7\gamma} O_{7\gamma} + C_{8g} O_{8g} \right) \right] + \text{h.c.}, \end{aligned} \quad (8)$$

where $V_{qb}V_{qs}^*$ ($q = u, c$ and t) are products of the Cabibbo-Kobayashi-Maskawa (CKM) matrix elements [25], C_i the Wilson coefficients, and O_i the relevant four-quark operators whose explicit forms could be found, for example, in Refs. [2, 24].

In recent years, QCDF has been employed extensively to study the B meson non-leptonic decays. For example, all of the decay modes considered here have been studied comprehensively within the SM in Refs. [2, 3, 4, 26]. The relevant decay amplitudes for $B \rightarrow \pi K$, πK^* and ρK decays within the QCDF formalism are shown in Appendix A. It is also noted that the framework contains estimates of some power-suppressed but numerically important contributions, such as the annihilation corrections. However, due to the appearance of endpoint divergence, these terms usually could not be computed rigorously. In Refs. [2, 3], to probe their possible effects conservatively, the endpoint divergent integrals are treated as signs of infrared sensitive contribution and phenomenological parameterized by

$$\int_0^1 \frac{dx}{x} \rightarrow X_A = (1 + \rho_A e^{i\phi_A}) \ln \frac{m_B}{\Lambda_h}, \quad \int_0^1 dy \frac{\ln y}{y} \rightarrow -\frac{1}{2}(X_A)^2 \quad (9)$$

with $\rho_A \leq 1$ and ϕ_A unrestricted. The different scenarios corresponding to different choices of ρ_A and ϕ_A have been thoroughly discussed in Ref. [3]. Although this way of parametrization seems reasonable, it is still very worthy to find some alternative schemes to regulate these endpoint divergences, as precise as possible, to estimate the strength and the associated strong phase in these power suppressed contributions.

It is interesting to note that recent theoretical and phenomenological studies are now accumulating supports for a softer infrared behavior of the gluon propagator [22, 27, 28]. Furthermore, an infrared finite dynamical gluon propagator, which is shown to be not divergent as fast as $\frac{1}{q^2}$, has been successfully applied to the B meson non-leptonic decays [29, 30]. Following these studies, in this paper we adopt the gluon propagator derived by Cornwall [20], to regulate the endpoint divergent integrals encountered within the QCDF formalism. The infrared finite gluon propagator is given by (in Minkowski space) [20]

$$D(q^2) = \frac{1}{q^2 - M_g^2(q^2) + i\epsilon}, \quad (10)$$

where q is the gluon momentum. The corresponding strong coupling constant reads

$$\alpha_s(q^2) = \frac{4\pi}{\beta_0 \ln \left(\frac{q^2 + 4M_g^2(q^2)}{\Lambda_{QCD}^2} \right)}, \quad (11)$$

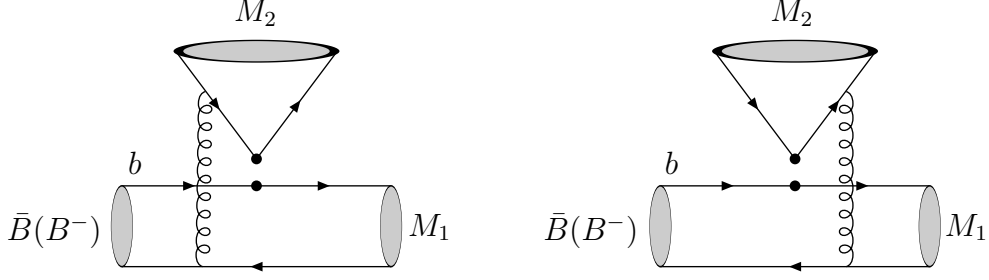


Figure 1: Feynman diagrams of hard spectator-scattering contributions.

where $\beta_0 = 11 - \frac{2}{3}n_f$ is the first coefficient of the beta function, and n_f the number of active flavors. The dynamical gluon mass $M_g^2(q^2)$ is obtained as [20]

$$M_g^2(q^2) = m_g^2 \left[\frac{\ln\left(\frac{q^2 + 4m_g^2}{\Lambda_{QCD}^2}\right)}{\ln\left(\frac{4m_g^2}{\Lambda_{QCD}^2}\right)} \right]^{-\frac{12}{11}}, \quad (12)$$

where m_g is the effective gluon mass, with a typical value $m_g = 500 \pm 200$ MeV, and $\Lambda_{QCD} = 225$ MeV.

2.1 Recalculate the hard-spectator scattering and the annihilation contributions

The next-to-leading order penguin contractions and vertex-type corrections to these decays are known free of infrared divergence and well-defined in QCDF [2, 3, 4], for which we would not repeat the calculation and concentrate on the hard-spectator scattering and the annihilation contributions. With the infrared finite gluon propagator to deal with the endpoint divergences, we will re-calculate the hard spectator and the annihilation corrections in $B \rightarrow PP$ and PV decays. The hard spectator scattering Feynman diagrams are shown in Fig. 1, where the spectator anti-quark goes from the \bar{B} meson to the final-state M_1 meson and the M_2 meson is emitted from the weak vertex. The longitudinal momentum fraction of the constituent quark in the $M_{2(1)}$ meson is denoted by x (y), and ξ is the light-cone momentum fraction of the light anti-quark in the B meson. To leading power in $1/m_b$, the hard spectator scattering contributions can be expressed as (where $x, y \gg \xi$ is assumed)

$$H_i(M_1 M_2) = \frac{B_{M_1 M_2}}{A_{M_1 M_2}} \int_0^1 dx dy d\xi \frac{\alpha_s(q^2)}{\xi} \Phi_{B1}(\xi) \Phi_{M_2}(x) \left[\frac{\Phi_{M_1}(y)}{\bar{x}(\bar{y} + \omega^2(q^2)/\xi)} + r_\chi^{M_1} \frac{\phi_{m_1}(y)}{x(\bar{y} + \omega^2(q^2)/\xi)} \right], \quad (13)$$

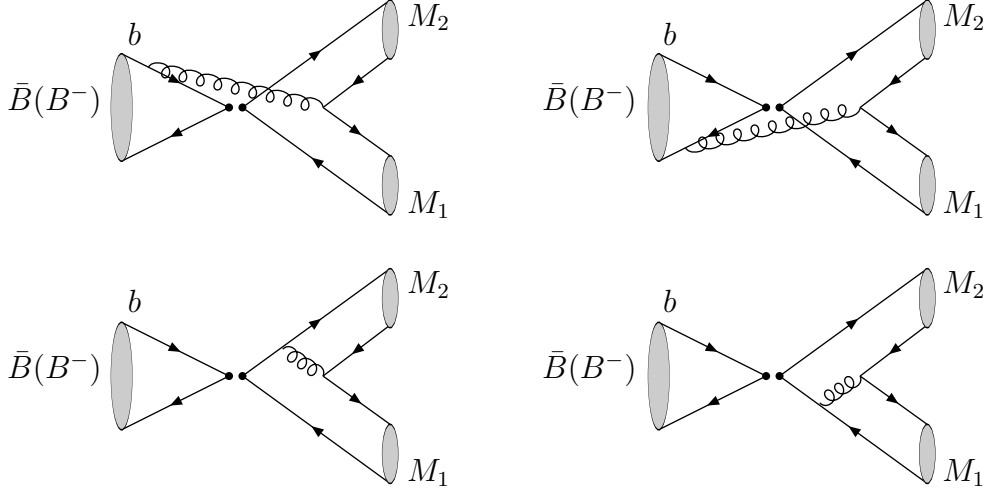


Figure 2: Feynman diagrams of weak annihilation contributions.

for the contributions of operators $Q_{i=1-4,9,10}$,

$$H_i(M_1 M_2) = -\frac{B_{M_1 M_2}}{A_{M_1 M_2}} \int_0^1 dx dy d\xi \frac{\alpha_s(q^2)}{\xi} \Phi_{B_1}(\xi) \Phi_{M_2}(x) \left[\frac{\Phi_{M_1}(y)}{x(\bar{y} + \omega^2(q^2)/\xi)} + r_\chi^{M_1} \frac{\phi_{m_1}(y)}{\bar{x}(\bar{y} + \omega^2(q^2)/\xi)} \right], \quad (14)$$

for $Q_{i=5,7}$, and $H_i(M_1 M_2) = 0$ for $Q_{i=6,8}$.

In the above Eqs. (13) and (14), $\Phi_{B_1}(\xi)$ is the B meson light-cone distribution amplitude(LCDA), $\Phi_{M_1}(x)$ and $\phi_{m_1}(y)$ are the twist-2 and the twist-3 LCDAs of light mesons, respectively, which are listed in Appendix B. $\omega^2(q^2) = M_g^2(q^2)/M_B^2$, $q^2 = -Q^2$ and $Q^2 \simeq -\xi\bar{y}M_B^2$ is the space-like gluon momentum square in the scattering kernels. The quantities $A_{M_1 M_2}$ and $B_{M_1 M_2}$ collect relevant constants which can be found in Ref. [3].

The Feynman diagrams of the weak annihilation topologies are shown in Fig. 2. When both M_1 and M_2 are pseudoscalars, the final decay amplitudes can be expressed as

$$A_1^i = \pi \int_0^1 dx dy \alpha_s(q^2) \left\{ \left[\frac{\bar{x}}{(\bar{x}y - \omega^2(q^2) + i\epsilon)(1 - x\bar{y})} + \frac{1}{(\bar{x}y - \omega^2(q^2) + i\epsilon)\bar{x}} \right] \Phi_{M_1}(y) \Phi_{M_2}(x) + \frac{2}{\bar{x}y - \omega^2(q^2) + i\epsilon} r_\chi^{M_1} r_\chi^{M_2} \phi_{m_1}(y) \phi_{m_2}(x) \right\}, \quad (15)$$

$$A_1^f = A_2^f = 0, \quad (16)$$

$$A_2^i = \pi \int_0^1 dx dy \alpha_s(q^2) \left\{ \left[\frac{y}{(\bar{x}y - \omega^2(q^2) + i\epsilon)(1 - x\bar{y})} + \frac{1}{(\bar{x}y - \omega^2(q^2) + i\epsilon)y} \right] \Phi_{M_1}(y) \Phi_{M_2}(x) + \frac{2}{\bar{x}y - \omega^2(q^2) + i\epsilon} r_\chi^{M_1} r_\chi^{M_2} \phi_{m_1}(y) \phi_{m_2}(x) \right\}, \quad (17)$$

$$A_3^i = \pi \int_0^1 dx dy \alpha_s(q^2) \left\{ \frac{2\bar{y}}{(\bar{x}y - \omega^2(q^2) + i\epsilon)(1 - x\bar{y})} r_\chi^{M_1} \phi_{m_1}(y) \Phi_{M_2}(x) - \frac{2x}{(\bar{x}y - \omega^2(q^2) + i\epsilon)(1 - x\bar{y})} r_\chi^{M_2}(x) \phi_{m_2}(x) \Phi_{M_1}(y) \right\}, \quad (18)$$

$$A_3^f = \pi \int_0^1 dx dy \alpha_s(q^2) \left\{ \frac{2(1 + \bar{x})}{(\bar{x}y - \omega^2(q^2) + i\epsilon)\bar{x}} r_\chi^{M_1} \phi_{m_1}(y) \Phi_{M_2}(x) + \frac{2(1 + y)}{(\bar{x}y - \omega^2(q^2) + i\epsilon)y} r_\chi^{M_2}(x) \phi_{m_2}(x) \Phi_{M_1}(y) \right\}, \quad (19)$$

where $q^2 \simeq \bar{x}yM_B^2$ is the time-like gluon momentum square. The ‘‘chirally-enhanced’’ factor r_χ^M is presented in Appendix B. The superscript ‘‘ i ’’ and ‘‘ f ’’ refer to the gluon emission from initial- and final-state quarks, respectively. The subscript ‘‘1’’, ‘‘2’’, and ‘‘3’’ correspond to three possible Dirac structure, with ‘‘1’’ for $(V - A) \otimes (V - A)$, ‘‘2’’ for $(V - A) \otimes (V + A)$, and ‘‘3’’ for $(S - P) \otimes (S + P)$, respectively. When M_1 is a vector meson and M_2 a pseudoscalar, the sign of the second term in A_1^i , the first term in A_2^i , and the second terms in A_3^i and A_3^f are needed to be changed. When M_2 is a vector meson and M_1 a pseudoscalar, one only has to change the overall sign of A_2^i .

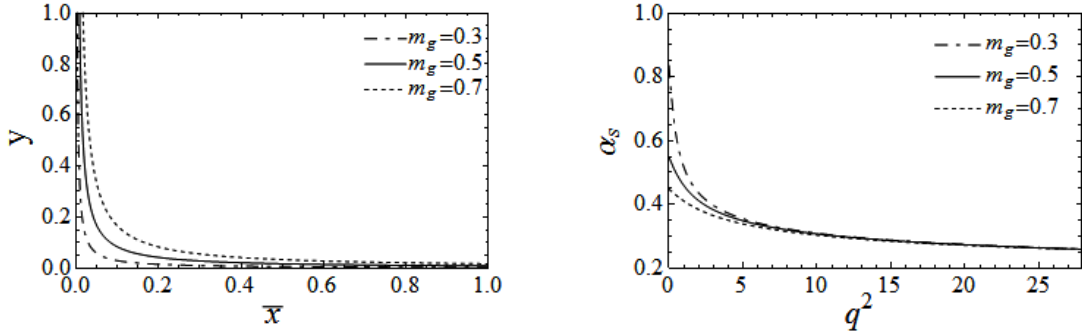


Figure 3: The singularities in integral spaces (left figure) in annihilation contributions and the variations of strong coupling constant corresponding to different m_g choices (in unit of GeV).

As shown by Eqs. (13) and (14) of the hard-spectator scattering contributions, the endpoint divergences are regulated by the infrared finite form of the gluon propagator. It is easy to observe from Eqs. (13) and (14) that hard-spectator scattering contributions are real. For the annihilation contributions shown by Eqs. (15)–(19), singularities of the time-like gluon propagators at the end-point of integrations (end-point divergence) are moved into integral

Table 1: The CP -averaged branching ratios (in units of 10^{-6}) of $B \rightarrow \pi K$, πK^* and ρK decays in SM with different m_g (in unit of GeV) are presented in QCDF columns.

Decay Mode	QCDF			Experiment
	$m_g = 0.3$	$m_g = 0.7$	$m_g = 0.45 \sim 0.55$	data
$B_u^- \rightarrow \pi^- \bar{K}^0$	44.4	16.8	23.17 ± 3.28	23.1 ± 1.0
$B_u^- \rightarrow \pi^0 K^-$	23.4	9.3	12.50 ± 1.65	12.9 ± 0.6
$\bar{B}_d^0 \rightarrow \pi^+ K^-$	44.7	16.3	22.71 ± 3.27	19.4 ± 0.6
$\bar{B}_d^0 \rightarrow \pi^0 \bar{K}^0$	21.2	7.3	10.50 ± 1.63	9.9 ± 0.6
$B_u^- \rightarrow \pi^- \bar{K}^{*0}$	28.3	5.2	8.90 ± 1.59	10.0 ± 0.8
$B_u^- \rightarrow \pi^0 K^{*-}$	15.2	3.4	5.25 ± 0.83	6.9 ± 2.3
$\bar{B}_d^0 \rightarrow \pi^+ K^{*-}$	28.7	5.3	9.13 ± 1.68	10.6 ± 0.9
$\bar{B}_d^0 \rightarrow \pi^0 \bar{K}^{*0}$	13.4	1.9	3.89 ± 0.82	2.4 ± 0.7
$B_u^- \rightarrow \rho^- \bar{K}^0$	31.8	5.6	10.27 ± 1.96	$8.0_{-1.4}^{+1.5}$
$B_u^- \rightarrow \rho^0 K^-$	14.9	2.5	4.81 ± 0.94	$3.81_{-0.46}^{+0.48}$
$\bar{B}_d^0 \rightarrow \rho^+ K^-$	38.6	8.0	13.42 ± 2.31	$8.6_{-1.1}^{+0.9}$
$\bar{B}_d^0 \rightarrow \rho^0 \bar{K}^0$	21.0	4.8	7.53 ± 1.25	$5.4_{-1.0}^{+0.9}$

intervals with the infrared finite form of the gluon propagator. Singularities in the integral intervals and variations of the effective strong coupling constant are shown in Fig. 3. It is noted that effective strong coupling constant is finite, but rather large in the small q^2 region. However, there is strong cancellations among the contributions of the small q^2 region nearby m_g^2 , which renders the annihilation contribution dominated by $q^2 > m_g^2$ region associated with a large imaginary part. This situation is quite similar to pQCD [15] where the large imaginary part from propagator regulated by k_T

$$\frac{1}{xym_B^2 - k_T^2 + i\epsilon} = P\left(\frac{1}{xym_B^2 - k_T^2}\right) - i\pi\delta(xym_B^2 - k_T^2), \quad (20)$$

and it is also found the power suppression of these terms relative to the leading contributions was not very significant, and important to account for CP violations in $B \rightarrow \pi K$ decays.

Table 2: The direct CP asymmetries (in unit of 10^{-2}) of $B \rightarrow \pi K$, πK^* and ρK decays in SM with different m_g (in unit of GeV). Other captions are the same as Table 1.

Decay Mode	QCDF			Experiment
	$m_g = 0.3$	$m_g = 0.7$	$m_g = 0.45 \sim 0.55$	data
$B_u^- \rightarrow \pi^- \bar{K}^0$	0.06	0.19	0.10 ± 0.08	0.9 ± 2.5
$B_u^- \rightarrow \pi^0 K^-$	-11.6	-8.3	-10.85 ± 0.84	5.0 ± 2.5
$\bar{B}_d^0 \rightarrow \pi^+ K^-$	-11.0	-11.4	-12.38 ± 0.69	-9.7 ± 1.2
$\bar{B}_d^0 \rightarrow \pi^0 \bar{K}^0$	2.5	0.1	1.39 ± 0.35	-14 ± 11
$B_u^- \rightarrow \pi^- \bar{K}^{*0}$	0.3	-0.0	0.16 ± 0.16	-11.4 ± 6.1
$B_u^- \rightarrow \pi^0 K^{*-}$	-27.0	-34.1	-41.20 ± 6.69	4 ± 29
$\bar{B}_d^0 \rightarrow \pi^+ K^{*-}$	-27.2	-47.6	-47.58 ± 8.42	-10 ± 11
$\bar{B}_d^0 \rightarrow \pi^0 \bar{K}^{*0}$	3.9	2.1	4.67 ± 1.14	-9_{-23}^{+32}
$B_u^- \rightarrow \rho^- \bar{K}^0$	0.1	1.2	0.53 ± 0.21	-12 ± 17
$B_u^- \rightarrow \rho^0 K^-$	28.1	49.7	46.27 ± 5.94	37 ± 11
$\bar{B}_d^0 \rightarrow \rho^+ K^-$	19.3	31.5	31.40 ± 4.63	15 ± 13
$\bar{B}_d^0 \rightarrow \rho^0 \bar{K}^0$	-4.2	0.2	-3.26 ± 1.29	-2 ± 29

2.2 The branching ratios and direct CP asymmetries in the SM

With the prescriptions for the endpoint divergences, we will present our numerical results of branching ratios and CP violations in these decays. Decay amplitudes and input parameters are listed in Appendices A and B, respectively. Our results are summarized in Table 1 and Table 2, where the relevant experimental data are also tabled for comparison.

In Table 1 (2), the experimental data column is the up-to-date averages for these branching ratios (direct CP violations) by HFAG [13]. It is shown that all the results are in good agreements with the experimental data with $m_g = 0.45 \sim 0.55$ GeV. It is also noted that the dynamical gluon mass $m_g = 0.45 \sim 0.55$ GeV are also consistent with findings in other phenomenal studies of B decays [29, 30] and the different solutions of SDE [20, 21, 22]. The phenomenology successes may indicate that the gluon mass, although not a directly measurable

quantity, furnishes a regulator for infrared divergences of QCD scattering processes.

From the CP averaged branching ratios in the fourth column of Table 1, we get

$$\begin{aligned} R_c &\equiv 2 \left[\frac{Br(B^- \rightarrow \pi^0 K^-)}{Br(B^- \rightarrow \pi^- K^0)} \right] = 1.08 \pm 0.30, \\ R_n &\equiv \frac{1}{2} \left[\frac{Br(\bar{B}^0 \rightarrow \pi^+ K^-)}{Br(\bar{B}^0 \rightarrow \pi^0 K^0)} \right] = 1.08 \pm 0.32, \end{aligned} \quad (21)$$

which agree with the experimental data $R_c = 1.12 \pm 0.10$ and $R_n = 0.98 \pm 0.09$ [13].

Table 2 is our results for direct CP violations. The fourth column is the results estimated with $m_g = 0.45 \sim 0.55$ GeV fixed by branching ratios, where the error-bars are simply due to the m_g variations. Compared with the experimental data, our results, except $A_{CP}(B_u^- \rightarrow \pi^0 K^-)$, agree with the measurements. For the most significant experimental result among the measurements of direct CP violations in the twelve decay modes $A_{CP}(\bar{B}_d^0 \rightarrow \pi^+ K^-) = -0.097 \pm 0.012$ [13], our result $A_{CP}(\bar{B}_d^0 \rightarrow \pi^+ K^-) = -0.124 \pm 0.007$ is in good agreement with it. As expected in the SM, we find again $A_{CP}(B_u^- \rightarrow \pi^0 K^-) = -0.108 \pm 0.008$ very close to $A_{CP}(\bar{B}_d^0 \rightarrow \pi^+ K^-)$, which are generally in agreement with the results of Refs. [3, 5, 6] listed in Eq. (5)–(7). So, it is very hard to accommodate the measured large difference between $A_{CP}(B_u^- \rightarrow \pi^0 K^-)$ and $A_{CP}(\bar{B}_d^0 \rightarrow \pi^+ K^-)$ in the SM with the available approaches for hadron-dynamics in B decays.

Although the problem could be due to hadronic effects unknown so far, the difference between $A_{CP}(B_u^- \rightarrow \pi^0 K^-)$ and $A_{CP}(\bar{B}_d^0 \rightarrow \pi^+ K^-)$ could be an indication of new sources of CP violation beyond the SM [18, 31, 32].

3 Possible resolution with new $(S+P) \otimes (S+P)$ operators

In this Section we will pursue possible NP solutions model-independently with a set of FCNC $(S+P) \otimes (S+P)$ operators. The effects of anomalous tensor and (pseudo-)scalar operators on hadronic B decays have attracted many attentions recently [31, 33, 34, 35, 36, 37]. For example, it is shown that they could help to resolve the abnormally large transverse polarizations observed in $B \rightarrow \phi K^*$ decay, as well as the large $Br(B \rightarrow \eta K^*)$ [36].

The general four-quark tensor operators can be expressed as

$$O_T^q = \bar{s} \sigma_{\mu\nu} (1 + \gamma_5) b \otimes \bar{q} \sigma^{\mu\nu} (1 + \gamma_5) q, \quad O_T^{q'} = \bar{s}_i \sigma_{\mu\nu} (1 + \gamma_5) b_j \otimes \bar{q}_j \sigma^{\mu\nu} (1 + \gamma_5) q_i, \quad (22)$$

which could be expressed, through the Fierz transformations, as linear combinations of the (pseudo-)scalar operators. In our present case, however, we find that the tensor operators with $q=u,d$ give the same contributions to the $B_u^- \rightarrow \pi^0 K^-$ and $B_d^0 \rightarrow \pi^+ K^-$ decays, so that they are hardly possible to resolve the direct CP violation difference, because after Fierz transformations, O_T^q and $O_T^{\prime q}$ with $q = u, d$ will give operators like $\bar{q}(1 + \gamma_5)b \otimes \bar{s}(1 + \gamma_5)q$ which are different from $\bar{s}(1 + \gamma_5)b \otimes \bar{s}(1 + \gamma_5)s$ of the Fierz transforming $O_T^s = \bar{s}\sigma_{\mu\nu}(1 + \gamma_5)b \otimes \bar{s}\sigma^{\mu\nu}(1 + \gamma_5)s$ for $B \rightarrow \phi K^*$ decays. On the other hand, the new operators like $\bar{s}(1 + \gamma_5)b \otimes \bar{q}(1 + \gamma_5)q$ may give a possible solution to ΔA because of their different contributions to the $B^- \rightarrow \pi^0 K^-$ and $\bar{B}^0 \rightarrow \pi^+ K^-$ decays.

We write the NP effective Hamiltonian for $b \rightarrow s$ transitions as

$$\mathcal{H}_{eff}^{NP} = \frac{G_F}{\sqrt{2}} \sum_{q=u,d} |V_{tb}V_{ts}^*| e^{i\delta_S^q} \left[C_{S1}^q O_{S1}^q + C_{S8}^q O_{S8}^q \right] + \text{h.c.} , \quad (23)$$

with O_{S1}^q and O_{S8}^q defined by

$$\begin{aligned} O_{S1}^u &= \bar{s}(1 + \gamma_5)b \otimes \bar{u}(1 + \gamma_5)u , & O_{S8}^u &= \bar{s}_i(1 + \gamma_5)b_j \otimes \bar{u}_j(1 + \gamma_5)u_i , \\ O_{S1}^d &= \bar{s}(1 + \gamma_5)b \otimes \bar{d}(1 + \gamma_5)d , & O_{S8}^d &= \bar{s}_i(1 + \gamma_5)b_j \otimes \bar{d}_j(1 + \gamma_5)d_i , \end{aligned} \quad (24)$$

where i and j are color indices. The coefficient $C_{S1(S8)}^q$ describes the relative interaction strength of the operator $O_{S1(S8)}^q$, and δ_S^q is their possible NP weak phase. Since both the coefficients and the weak phase are unknown parameters, for simplicity, we shall only consider their leading contributions with the naive factorization(NF) approximation.

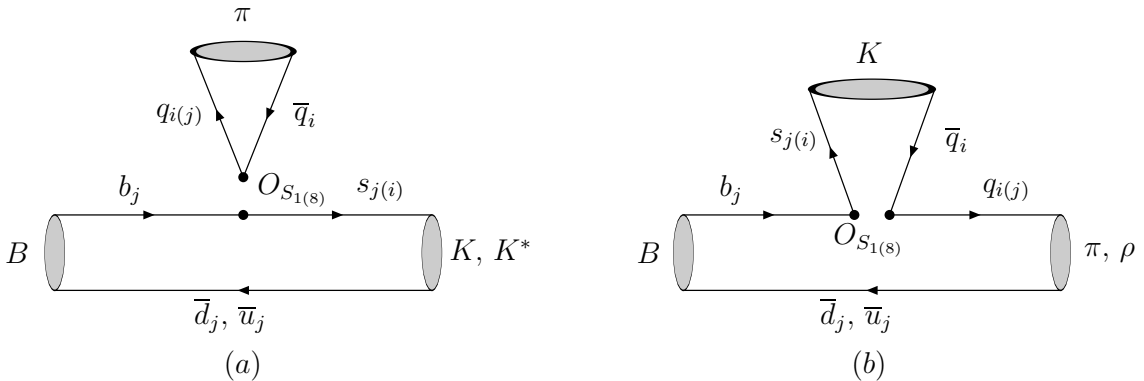


Figure 4: Feynman diagrams contributing to the amplitudes of $B \rightarrow \pi K, \pi K^*$ and ρK decays due to the $(S + P) \otimes (S + P)$ operators.

The relevant Feynman diagrams of the NP operators are shown in Fig. 4 with $q = u, d$. With the NF approximation, it is easy to see that, for the $B \rightarrow \pi^0 K^{*-}$ and $\pi^0 \bar{K}^{*0}$ decay modes, only Fig. 4 (a) contributes, for the $B \rightarrow \pi^- \bar{K}^0$, $\pi^+ K^-$ and ρK decay modes, only Fig. 4 (b) contributes, while both topology structures contribute to the $B \rightarrow \pi^0 K^-$ and $\pi^0 \bar{K}^0$ decay modes. However, none of them contributes to $B \rightarrow \pi^- K^{*0}$ and $\pi^+ K^{*-}$ decays. After some simple calculations, these NP contributions to the decay amplitudes of the $B \rightarrow \pi K$, πK^* and ρK decays are obtained as

$$\mathcal{A}_{B^- \rightarrow \pi^- \bar{K}^0}^{\text{NP}} = i \frac{G_F}{\sqrt{2}} \frac{1}{4} |V_{tb} V_{ts}^*| m_{B_u}^2 e^{i\delta_S^d} g_S^d r_\chi^K F_0^{B \rightarrow \pi}(m_K^2) f_K, \quad (25)$$

$$\begin{aligned} \mathcal{A}_{B^- \rightarrow \pi^0 K^-}^{\text{NP}} &= i \frac{G_F}{\sqrt{2}} \frac{1}{4\sqrt{2}} |V_{tb} V_{ts}^*| m_{B_u}^2 \left[e^{i\delta_S^u} g_S^u r_\chi^K F_0^{B \rightarrow \pi}(m_K^2) f_K \right. \\ &\quad \left. - 2(e^{i\delta_S^u} g_S^{lu} - e^{i\delta_S^d} g_S^{ld}) r_\chi^\pi F_0^{B \rightarrow K}(m_\pi^2) f_\pi \right], \end{aligned} \quad (26)$$

$$\mathcal{A}_{\bar{B}^0 \rightarrow \pi^+ K^-}^{\text{NP}} = i \frac{G_F}{\sqrt{2}} \frac{1}{4} |V_{tb} V_{ts}^*| m_{B_d}^2 e^{i\delta_S^u} g_S^u r_\chi^K F_0^{B \rightarrow \pi}(m_K^2) f_K, \quad (27)$$

$$\begin{aligned} \mathcal{A}_{\bar{B}^0 \rightarrow \pi^0 \bar{K}^0}^{\text{NP}} &= i \frac{G_F}{\sqrt{2}} \frac{1}{4\sqrt{2}} |V_{tb} V_{ts}^*| m_{B_d}^2 \left[-e^{i\delta_S^d} g_S^d r_\chi^K F_0^{B \rightarrow \pi}(m_K^2) f_K \right. \\ &\quad \left. - 2(e^{i\delta_S^u} g_S^{lu} - e^{i\delta_S^d} g_S^{ld}) r_\chi^\pi F_0^{B \rightarrow K}(m_\pi^2) f_\pi \right], \end{aligned} \quad (28)$$

$$\mathcal{A}_{B^- \rightarrow \pi^- \bar{K}^{*0}}^{\text{NP}} = 0, \quad (29)$$

$$\mathcal{A}_{B^- \rightarrow \pi^0 K^{*-}}^{\text{NP}} = i \frac{G_F}{\sqrt{2}} \frac{1}{2\sqrt{2}} |V_{tb} V_{ts}^*| m_{B_u}^2 \left[e^{i\delta_S^u} g_S^{lu} - e^{i\delta_S^d} g_S^{ld} \right] r_\chi^\pi A_0^{B \rightarrow K^*}(m_\pi^2) f_\pi, \quad (30)$$

$$\mathcal{A}_{\bar{B}^0 \rightarrow \pi^+ K^{*-}}^{\text{NP}} = 0, \quad (31)$$

$$\mathcal{A}_{\bar{B}^0 \rightarrow \pi^0 \bar{K}^{*0}}^{\text{NP}} = i \frac{G_F}{\sqrt{2}} \frac{1}{2\sqrt{2}} |V_{tb} V_{ts}^*| m_{B_u}^2 \left[e^{i\delta_S^u} g_S^{lu} - e^{i\delta_S^d} g_S^{ld} \right] r_\chi^\pi A_0^{B \rightarrow K^*}(m_\pi^2) f_\pi, \quad (32)$$

$$\mathcal{A}_{B^- \rightarrow \rho^- \bar{K}^0}^{\text{NP}} = -i \frac{G_F}{\sqrt{2}} \frac{1}{4} |V_{tb} V_{ts}^*| m_{B_u}^2 e^{i\delta_S^d} g_S^d r_\chi^K A_0^{B \rightarrow \rho}(m_K^2) f_K, \quad (33)$$

$$\mathcal{A}_{B^- \rightarrow \rho^0 K^-}^{\text{NP}} = -i \frac{G_F}{\sqrt{2}} \frac{1}{4\sqrt{2}} |V_{tb} V_{ts}^*| m_{B_u}^2 e^{i\delta_S^u} g_S^u r_\chi^K A_0^{B \rightarrow \rho}(m_K^2) f_K, \quad (34)$$

$$\mathcal{A}_{\bar{B}^0 \rightarrow \rho^+ K^-}^{\text{NP}} = -i \frac{G_F}{\sqrt{2}} \frac{1}{4} |V_{tb} V_{ts}^*| m_{B_u}^2 e^{i\delta_S^u} g_S^u r_\chi^K A_0^{B \rightarrow \rho}(m_K^2) f_K, \quad (35)$$

$$\mathcal{A}_{\bar{B}^0 \rightarrow \rho^0 \bar{K}^0}^{\text{NP}} = i \frac{G_F}{\sqrt{2}} \frac{1}{4\sqrt{2}} |V_{tb} V_{ts}^*| m_{B_u}^2 e^{i\delta_S^d} g_S^d r_\chi^K A_0^{B \rightarrow \rho}(m_K^2) f_K, \quad (36)$$

where

$$\begin{aligned} g_S^u &= C_{S1}^u + \frac{1}{N_c} C_{S8}^u, & g_S^u &= C_{S8}^u + \frac{1}{N_c} C_{S1}^u, \\ g_S^d &= C_{S1}^d + \frac{1}{N_c} C_{S8}^d, & g_S^d &= C_{S8}^d + \frac{1}{N_c} C_{S1}^d. \end{aligned} \quad (37)$$

Comparing the NP amplitudes Eq. (26) with Eq. (27), we expect that these new (pseudo-)scalar operators might provide a possible resolution to the direct CP violation difference, which is realized in the following numerical analyses.

3.1 Numerical analyses and discussions of new pseudo-scalar operators

Our analysis consists of five cases with different assumptions for dominance of NP operators, namely,

- Case I: $b \rightarrow su\bar{u}$ operators O_{S1}^u and O_{S8}^u ,
- Case II: $b \rightarrow sdd\bar{d}$ operators O_{S1}^d and O_{S8}^d ,
- Case III: $b \rightarrow sdd\bar{d}$ operator O_{S1}^d solely,
- Case IV: only color singlet operators O_{S1}^u and O_{S1}^d ,
- Case V: all the operators O_{S1}^u , O_{S8}^u , O_{S1}^d and O_{S8}^d .

For each case, the corresponding effective Hamiltonian could be read from Eq. (23). It could be expected that a collection of related decay modes could constrain the relevant NP parameter spaces restrictively.

Our fitting is performed with the experimental data varying randomly within their 2σ error-bars, while the theoretical uncertainties are obtained by varying the input parameters within the regions specified in Appendix B. Our numerical results are summarized in Table 3–5 where the assigned uncertainties of our fitting results should be understood at 2σ statistical level. Illustratively, the constrained NP parameter spaces are shown in Figs. 5–9, respectively. It is noted that, to leading order approximation, both $B_u^- \rightarrow \pi^- \bar{K}^{*0}$ and $\bar{B}_d^0 \rightarrow \pi^+ \bar{K}^{*-}$ decays do not receive these NP contributions, so we perform fitting for the remained ten decay modes. In the following, we present numerical analyses subdivided into five cases.

Case I: $b \rightarrow su\bar{u}$ operators O_{S1}^u and O_{S8}^u

We just take into account the contributions of O_{S1}^u and O_{S8}^u in Eq. (23), *i.e.* $C_{S1}^d = C_{S8}^d = 0$. In this case, we take the branching ratios of the seven relevant decays $B_u^- \rightarrow \pi^0 K^-$, $\pi^0 K^{*-}$,

Table 3: The CP -averaged branching ratios (in units of 10^{-6}) in different NP Cases with $m_g = 0.5\text{GeV}$. The dash means (pseudo-)scalar operators of the Case irrelevant to the corresponding decay mode.

Decay Mode	Experiment	NP				
	data	Case I	Case II	Case III	Case IV	Case V
$B_u^- \rightarrow \pi^- \bar{K}^0$	23.1 ± 1.0	—	23.0 ± 1.0	22.9 ± 0.9	21.5 ± 0.3	22.4 ± 0.9
$B_u^- \rightarrow \pi^0 K^-$	12.9 ± 0.6	12.1 ± 0.4	12.8 ± 0.7	12.7 ± 0.6	12.1 ± 0.3	12.1 ± 0.4
$\bar{B}_d^0 \rightarrow \pi^+ K^-$	19.4 ± 0.6	20.2 ± 0.3	—	—	20.4 ± 0.2	20.1 ± 0.4
$\bar{B}_d^0 \rightarrow \pi^0 \bar{K}^0$	9.9 ± 0.6	9.0 ± 0.3	9.9 ± 0.6	10.0 ± 0.7	9.0 ± 0.2	9.1 ± 0.4
$B_u^- \rightarrow \pi^0 K^{*-}$	6.9 ± 2.3	4.2 ± 0.2	4.4 ± 0.4	4.4 ± 0.4	4.3 ± 0.3	4.3 ± 0.3
$\bar{B}_d^0 \rightarrow \pi^0 \bar{K}^{*0}$	2.4 ± 0.7	3.4 ± 0.3	3.5 ± 0.2	3.5 ± 0.2	3.1 ± 0.3	2.9 ± 0.2
$B_u^- \rightarrow \rho^- \bar{K}^0$	$8.0_{-1.4}^{+1.5}$	—	8.6 ± 0.7	8.6 ± 0.7	7.4 ± 0.4	7.1 ± 0.4
$B_u^- \rightarrow \rho^0 K^-$	$3.81_{-0.46}^{+0.48}$	3.4 ± 0.2	—	—	3.4 ± 0.2	3.4 ± 0.2
$\bar{B}_d^0 \rightarrow \rho^+ K^-$	$8.6_{-1.1}^{+0.9}$	9.7 ± 0.5	—	—	9.7 ± 0.5	9.8 ± 0.5
$\bar{B}_d^0 \rightarrow \rho^0 \bar{K}^0$	$5.4_{-1.0}^{+0.9}$	—	6.5 ± 0.4	6.5 ± 0.4	5.5 ± 0.3	5.4 ± 0.4

$\rho^0 K^-$ and $\bar{B}_d^0 \rightarrow \pi^+ K^-$, $\pi^0 \bar{K}^0$, $\pi^0 \bar{K}^{*0}$, $\rho^+ K^-$ as constraints and leave the direct CP asymmetries as our predictions. The allowed regions of the NP parameters C_{S1}^u , C_{S8}^u and δ_S^u are shown in Fig. 5. From which, we find the spaces of C_{S1}^u and δ_S^u consist of two parts (dark and gray). However, with the gray part, we get $A_{CP}(B_u^- \rightarrow \pi^0 K^-) = -0.154 \pm 0.038$ which conflicts with experimental data 0.050 ± 0.025 . So, the gray region should be excluded. With the dark part of parameter spaces, our prediction $A_{CP}(B_u^- \rightarrow \pi^0 K^-) = 0.088 \pm 0.064$ is consistent with experimental data. Furthermore, the branching ratios and direct CP asymmetries of the other decay modes, listed in the third column of Table 3 and 4, agree with experimental data within error bars. The constrained parameter space C_{S1}^u , C_{S8}^u and δ_S^u are listed in the second column of Table 5. We note that $C_{S1}^u \approx -C_{S8}^u \approx -0.04$ with $\delta_S^u \approx 100^\circ$, it means the strength of color-singlet and color-octet operators are similar, however, such a situation may be hard to be generated with a realistic available NP model.

Table 4: The direct CP asymmetries (in unit of 10^{-2}) of $B \rightarrow \pi K, \pi K^*$ and ρK decays. Other captions are the same as Table 3

Decay Mode	Experiment	NP				
	data	Case I	Case II	Case III	Case IV	Case V
$B_u^- \rightarrow \pi^- \bar{K}^0$	0.9 ± 2.5	—	1.7 ± 2.9	2.0 ± 0.2	3.9 ± 1.0	3.2 ± 1.3
$B_u^- \rightarrow \pi^0 K^-$	5.0 ± 2.5	8.8 ± 6.4	1.1 ± 0.9	1.2 ± 0.9	2.8 ± 5.5	1.8 ± 1.3
$\bar{B}_d^0 \rightarrow \pi^+ K^-$	-9.7 ± 1.2	-5.7 ± 4.4	—	—	-10.0 ± 0.8	-9.2 ± 1.3
$\bar{B}_d^0 \rightarrow \pi^0 \bar{K}^0$	-14 ± 11	-18.6 ± 7.5	-12.8 ± 3.9	-12.6 ± 1.6	-10.2 ± 7.0	-8.2 ± 2.8
$B_u^- \rightarrow \pi^0 K^{*-}$	4 ± 29	4.2 ± 19.3	-8.1 ± 3.3	-8.0 ± 3.3	-4.9 ± 19.7	-13.2 ± 4.6
$\bar{B}_d^0 \rightarrow \pi^0 \bar{K}^{*0}$	-9_{-23}^{+32}	-61.7 ± 22.0	-49.9 ± 3.4	-49.8 ± 3.8	-52.8 ± 24.2	-47.0 ± 6.5
$B_u^- \rightarrow \rho^- \bar{K}^0$	-12 ± 17	—	-5.9 ± 10.9	-6.5 ± 0.8	-15.1 ± 4.2	-13.1 ± 5.9
$B_u^- \rightarrow \rho^0 K^-$	37 ± 11	32.8 ± 16.5	—	—	48.3 ± 3.5	43.9 ± 5.2
$\bar{B}_d^0 \rightarrow \rho^+ K^-$	15 ± 13	19.2 ± 12.9	—	—	31.9 ± 2.7	28.0 ± 4.1
$\bar{B}_d^0 \rightarrow \rho^0 \bar{K}^0$	-2 ± 29	—	-8.1 ± 8.1	-8.5 ± 0.9	-14.9 ± 3.0	-13.5 ± 4.4

Table 5: The numerical results for the parameters $C_{S1}^u, C_{S1}^d, \delta_S^u, C_{S1}^d, C_{S8}^d$ and δ_S^d in different NP Cases. The dashes mean the corresponding operators are neglected in the Case.

NP para.	Case I	Case II	Case III	Case IV	Case V
$C_{S1}^u (\times 10^{-3})$	-41.6 ± 13.4	—	—	25.8 ± 8.4	-6.7 ± 10.5
$C_{S8}^u (\times 10^{-3})$	38.7 ± 18.2	—	—	—	16.0 ± 7.1
δ_S^u	$99.5^\circ \pm 6.1^\circ$	—	—	$107.0^\circ \pm 11.5^\circ$	$73.0^\circ \pm 23.8^\circ$
$C_{S1}^d (\times 10^{-3})$	—	23.0 ± 5.1	22.8 ± 2.3	50.3 ± 12.8	17.5 ± 10.1
$C_{S8}^d (\times 10^{-3})$	—	-0.8 ± 13.7	—	—	10.5 ± 9.4
δ_S^d	—	$100.0^\circ \pm 8.7^\circ$	$99.3^\circ \pm 9.2^\circ$	$106.6^\circ \pm 7.3^\circ$	$114.7^\circ \pm 18.6^\circ$

Case II: $b \rightarrow s d \bar{d}$ operators O_{S1}^d and O_{S8}^d

In a large category of NP scenarios with scalar interactions, for example, two-Higgs doublets model II, down type fermion Yukawa couplings are enhanced. So, in this case, we evaluate the

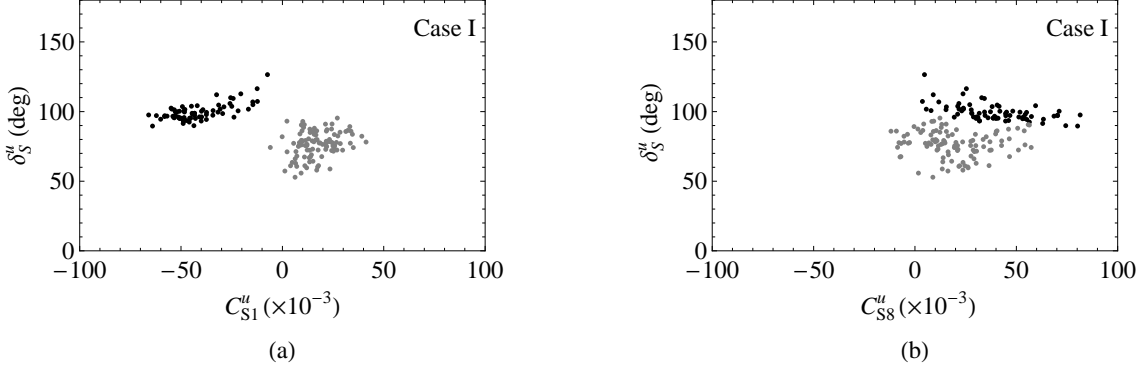


Figure 5: The allowed regions for the parameters C_{S1}^u , C_{S8}^u and δ_S^u of Case I.

effects of O_{S1}^d and O_{S8}^d and neglect O_{S1}^u and O_{S8}^u .

As shown by Eqs. (25)–(36), $O_{S1(8)}^d$ contributes to the decays $B \rightarrow \pi^- \bar{K}^0$, $\pi^0 K^-$, $\pi^0 K^{*-}$, $\rho^- \bar{K}^0$, $\pi^0 \bar{K}^0$, $\pi^0 \bar{K}^{*0}$, and $\rho^0 \bar{K}^0$. From Table 1, one can find that the SM predictions for their branching ratios are consistent with the experimental data. So, in this Case, NP weak phase δ_S^d would be arbitrary for very small strengths of C_{S1}^d and C_{S8}^d , we thus have to take into account both branching ratios and direct CP violations as constraints. The allowed region of C_{S1}^d , C_{S8}^d and δ_S^d are shown in Fig. 6. The fitted results are shown in the fourth column of Table 3, 4 and the third column of Table 5. Interestingly, we note that $C_{S1}^d = 0.023 \pm 0.005$, $C_{S8}^d = -0.001 \pm 0.013$ (consistent with zero) with $\delta_S^d \approx 100^\circ$. It indicates that color-singlet operator O_{S1}^d dominates the NP $b \rightarrow s d \bar{d}$ contributions. Actually, with O_{S1}^d only, we could find a solution to the “ πK puzzle” which will be discussed in next Case.

Compared with Case I, it is found that $|C_{S1}^d| < |C_{S1}^u| \approx |C_{S8}^u|$. However, we can’t conclude that $O_{S1(8)}^u$ dominates the NP contribution until we consider the two operators simultaneously, which will be discussed in coming Case IV and Case V.

Case III: $b \rightarrow s d \bar{d}$ operator O_{S1}^d solely

As the former Case, both branching ratio and direct CP violation are taken as constraints. With O_{S1}^d solely, we find a solution to the “ πK puzzle” with the C_{S1}^d and δ_S^d allowed region shown in Fig. 7. The numerical results are listed in fifth column of Table 3, 4 and fourth column of Table 5, respectively. C_{S1}^d and δ_S^d are found similar to the ones of Case II. It confirms our findings in Case II that O_{S1}^d dominates the NP contributions and the contribution of O_{S8}^d is

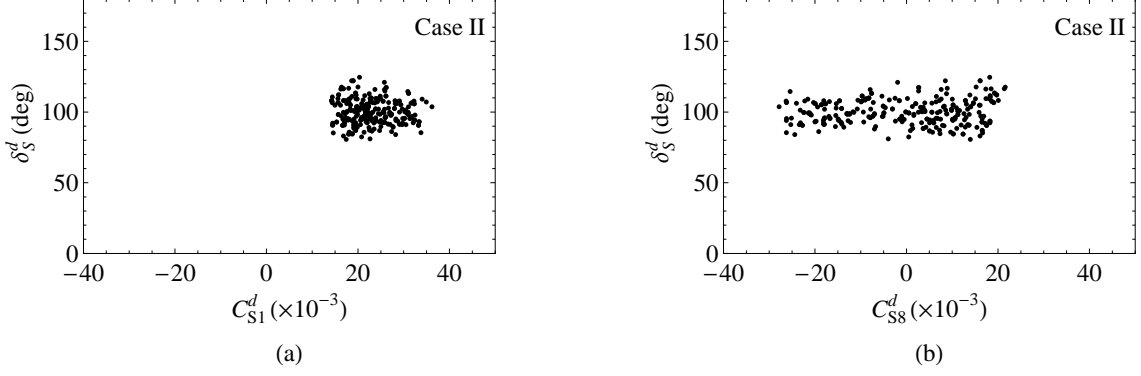


Figure 6: The allowed regions for the parameters C_{S1}^d , C_{S8}^d and δ_S^d in Case II with $m_g = 0.5$ GeV.

negligible. As known, it is easy to generate the situation in many NP scenarios. However, both the strength $C_{S1}^d \approx 0.022$ and the new weak phase $\delta^d \approx 99^\circ$ normalized to $\frac{G_F}{\sqrt{2}}|V_{tb}V_{ts}^*|$ may be toughly large for realistic NP models without violating other precise electro-weak measurements.

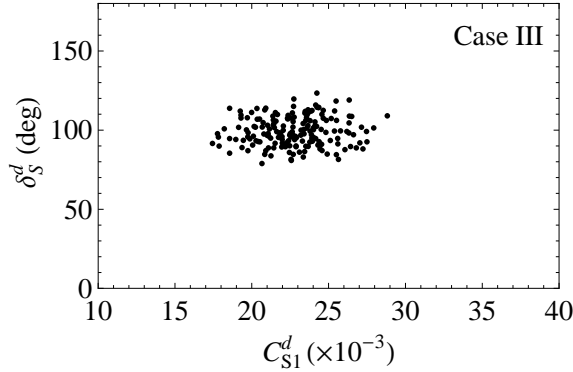


Figure 7: The allowed regions for the parameters C_{S1}^d and δ_S^d of Case III.

Case IV: only color-singlet operators O_{S1}^u and O_{S1}^d

In order to compare the relative strength of two color singlet operators O_{S1}^d and O_{S1}^u , we take them into account at the same time and neglect the other two color-octet ones. Taking the branching ratios of the relevant decays as constraints, we find the allowed regions for the NP parameters C_{S1}^u , δ_S^u , C_{S1}^d and δ_S^d , which are shown in Fig. 8. All our predictions for the direct CP violations, listed in in sixth column of Table 4, agree with experimental data. Especially, we note our predictions $A_{CP}(B^- \rightarrow \pi^0 K^-) = 0.028 \pm 0.055$ and $\Delta A = 0.128 \pm 0.056$ agree with

experimental data very well.

The fifth column of Table 5 is the parameter space obtained for the present Case. We find that strength of C_{S1}^d in Case IV is larger than the ones in Case II and Case III, because the terms of C_{S1}^d and C_{S1}^u always have opposite sign in Eqs. (26), (28), (30) and (32), but only one of them exists in the other decay modes. It is found that $C_{S1}^d \approx 2 \times C_{S1}^u \approx 0.05$ with $\delta_S^d \approx \delta_S^u \approx 107^\circ$, which shows O_{S1}^d dominance.

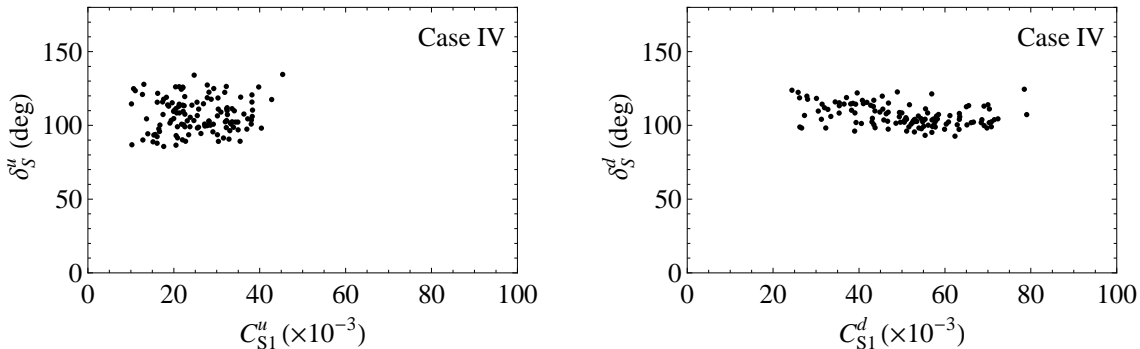


Figure 8: The allowed regions for the parameters C_{S1}^u , δ_S^u , C_{S1}^d and δ_S^d of Case IV.

Case V: all the operators O_{S1}^u , O_{S8}^u , O_{S1}^d and O_{S8}^d

At last, we fit the measured branching ratios and the direct CP violations of all the relevant ten decay models with the four operators in Eq. (24). Generally the ten CP averaged branching ratios are measured with high significant, however, only $A_{CP}(B^0 \rightarrow \pi^\pm K^\mp)$ is well established at 8σ level and $A_{CP}(B_u^- \rightarrow \pi^0 K^-)$ by itself is at 2σ level only.

From the fit, the allowed regions for the six NP parameters C_{S1}^u , C_{S8}^u , δ_S^u , C_{S1}^d , C_{S8}^d and δ_S^d shown in Fig. 9. The fitted branching ratios and CP violations are listed in the seventh column of Table 3 and 4, and the fitted values of the NP parameters are presented in the last column of Table 5, respectively. Since the experimental data are allowed varying randomly within their 2σ error-bars, the uncertainties of our fitting results are turned to be quite large.

We find $C_{S1}^u = (-6.7 \pm 10.5) \times 10^{-3}$ and $C_{S8}^u = (16.0 \pm 7.1) \times 10^{-3}$ with $\delta_S^u = 73.0^\circ \pm 23.8^\circ$, which shift our predication $A_{CP}(\bar{B}^0 \rightarrow \pi^\pm K^\mp) \approx -0.124$ in the SM more closer to the experimental data -0.097 . However, it does not indicate that the $b \rightarrow su\bar{u}$ operators are important for resolving CP violation difference ΔA , since the sum of their contributions to $B^- \rightarrow \pi^0 K^-$ is quite small due to cancellation among them. For the $b \rightarrow s\bar{d}d$ operators, we

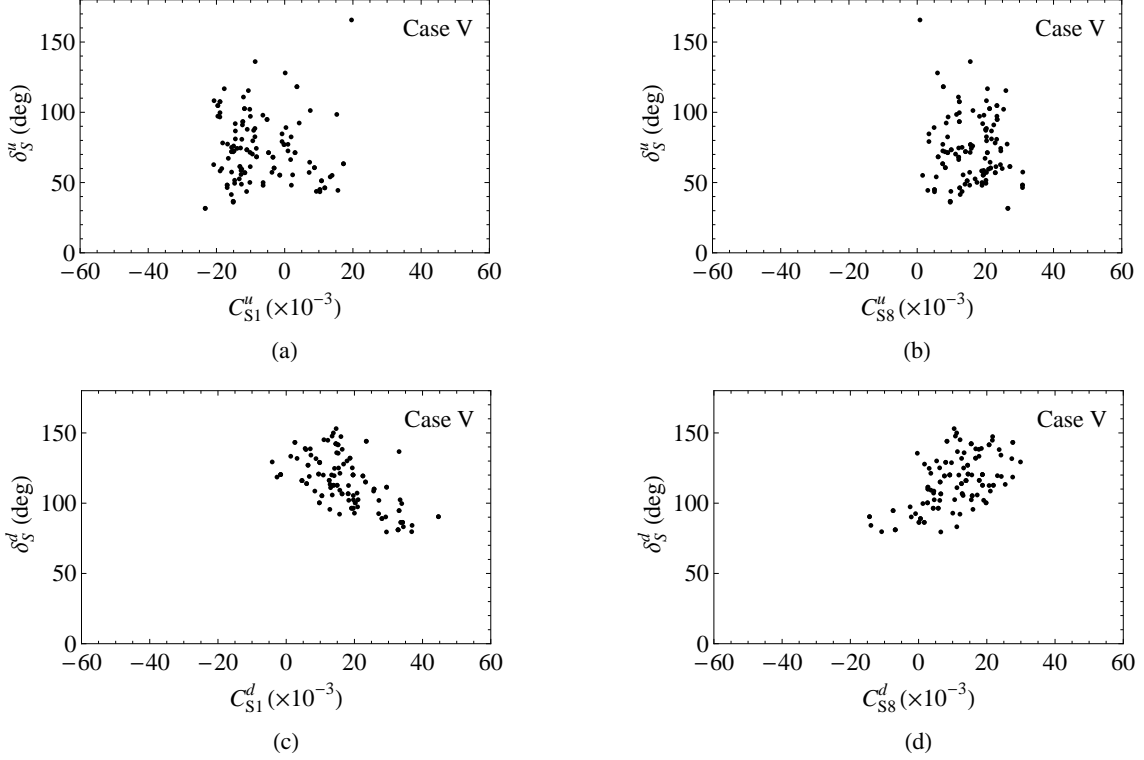


Figure 9: The allowed regions for the parameters C_{S1}^u , C_{S8}^u , δ_S^u , C_{S1}^d , C_{S8}^d and δ_S^d of Case V.

get $C_{S1}^d = (17.5 \pm 10.1) \times 10^{-3}$ and $C_{S8}^d = (10.5 \pm 9.4) \times 10^{-3}$ with $\delta_S^d = 114.7^\circ \pm 18.6^\circ$. The results are consistent with these of Case II and Case III as shown in Table 5, however, due to interferences with $b \rightarrow su\bar{u}$ contributions, the uncertainties are much larger than the two former Cases where $b \rightarrow su\bar{u}$ operators are dropped. Moreover, as shown by Eq. (26), C_{S8}^d is suppressed by $1/N_c$ in the amplitude of $B^- \rightarrow \pi^0 K^-$, thus, the dominate status of O_{S1}^d for resolving ΔA is remained.

3.2 The mixing-induced CP asymmetries in $B \rightarrow \pi^0 K_S$ and $B \rightarrow \rho^0 K_S$

So far we have discussed the direct CP asymmetries in the these decays with five NP scenarios. However, it is naturally to question if we can account for the mixing-induced CP asymmetries in $\bar{B}^0 \rightarrow \pi^0 K_S$ and $\rho^0 K_S$ decays with these constrained parameter spaces obtained in the former subsection. As known, the mixing-induced asymmetries are more suitable for probing new physics effects entered via $b \rightarrow sq\bar{q}$ parton processes than the direct ones, since the former ones

Table 6: The mixing-induced CP asymmetries (in unit of 10^{-2}) of $\bar{B}^0 \rightarrow \pi^0 K_S, \rho^0 K_S$ decays. Other captions are the same as Table 3

Decay Mode	Experiment	SM	NP				
			Case I	Case II	Case III	Case IV	Case V
	data						
$\bar{B}_d^0 \rightarrow \pi^0 K_S$	38 ± 19	77 ± 4	45 ± 11	56 ± 5	57 ± 3	59 ± 9	62 ± 8
$\bar{B}_d^0 \rightarrow \rho^0 K_S$	61_{-27}^{+25}	66 ± 3	—	61 ± 6	61 ± 3	56 ± 3	57 ± 4

could be predicted more accurately in QCDF. Detail discussions for the interesting feature could be found in Ref. [38]. Recently, the measured relative small mixing-induced asymmetry (with large error-bar) in $\bar{B}^0 \rightarrow \pi^0 K_S$ has attracted much attention in the literature [38, 39, 40, 18, 41].

The time-dependent CP asymmetries in $\bar{B}^0 \rightarrow \pi^0 K_S$ and $\rho^0 K_S$ decays could be written as

$$\mathcal{A}_f(t) = S_f \sin(\Delta m_d t) - C_f \cos(\Delta m_d t), \quad (38)$$

where $-C_f \equiv \mathcal{A}_{CP}$ is the direct CP violation already discussed in former subsection. $S_f = \mathcal{A}_{CP}^{mix}$ is the mixing-induced asymmetry

$$A_{CP}^{mix}(\bar{B}^0 \rightarrow f) = \frac{2\text{Im}\lambda_f}{1 + |\lambda_f|^2} \quad (f = \pi^0 K_S, \rho^0 K_S, \quad \eta_f = -1) \quad (39)$$

where $\lambda_f = -e^{-2i\beta} \bar{A}^{00}/A^{00}$ and $\sin(2\beta) = \sin(2\beta)_{\Psi K_S} = 0.68 \pm 0.03$ [13], since the NP operators are irrelevant to $B^0 - \bar{B}^0$ mixing amplitude.

Using the constrained parameters of the NP operators in Table 5 and taking $m_g = 0.5$ GeV, our numerical results are listed in Table 6 for the SM and the five Cases of NP operators. The experimental data column is the averages by HFAG [13]. In the SM, up to doubly Cabibbo suppressed amplitudes, one can expect

$$\mathcal{A}_{CP} \approx 0, \quad \mathcal{A}_{CP}^{mix} = S \approx \sin(2\beta)_{\Psi K_S} = 0.68 \pm 0.03 \quad (40)$$

for the two decay modes. We get $A_{CP}^{mix}(\pi^0 K_S) = 0.77 \pm 0.04$ and $A_{CP}^{mix}(\rho^0 K_S) = 0.66 \pm 0.03$. It is noted that the former is slight larger than $\sin(2\beta)_{\Psi K_S}$ which is due to corrections of the suppressed amplitudes proportional to $V_{ub}V_{us}^*$ as discussed in Ref.[38]¹. As shown in Table.6,

¹ If the old data $\sin(2\beta)_{\Psi K_S} = 0.725 \pm 0.037$ used, we get $\Delta S_{\pi^0 K_S} = S_{\pi^0 K_S} - \sin(2\beta)_{\Psi K_S} = 0.05 \pm 0.08$ and

the NP pseudoscalar operators decrease $S_{\pi^0 K_S}$ and $S_{\rho^0 K_S}$ (weaker than former), which seems to be favored by the experimental data.

We note that HFAG has not included the following data yet

$$A_{CP}^{mix}(\bar{B}^0 \rightarrow \pi^0 K_S) = 0.55 \pm 0.20 \pm 0.03 \quad \text{BABAR [42]}, \quad (41)$$

$$A_{CP}^{mix}(\bar{B}^0 \rightarrow \pi^0 K_S) = 0.67 \pm 0.31 \pm 0.08 \quad \text{Belle [43]}, \quad (42)$$

which are reported very recently at ICHEP08. The average reads $A_{CP}^{mix}(\bar{B}^0 \rightarrow \pi^0 K_S) = 0.58 \pm 0.17$. Again from Table 6, we find the outputs of all the five Cases with their fitted parameter spaces are in good agreements with the new experimental results since the error-bar are still large. Taking Case II as example, i.e., assuming NP from $b \rightarrow s\bar{d}\bar{d}$, we present the correlations of the direct and the mixing-induced CP asymmetries for $\bar{B}^0 \rightarrow \pi^0 K_S$ and $\bar{B}^0 \rightarrow \rho^0 K_S$ decays in Fig. 10, where the constrained parameters listed in Table 5 are used. Although all points fall in the present experimental error-bars, Fig. 10 shows interesting correlations between A_{CP}^{dir} and $A_{CP}^{mix}(S)$. If the experimental $S_{\pi^0 K_S}$ shrank to be much lower than $\sin(2\beta)_{\Psi K_S}$, the NP Case II would give large negative direct CP asymmetry. Similar implication also applies to $\rho^0 K_S$ final states.

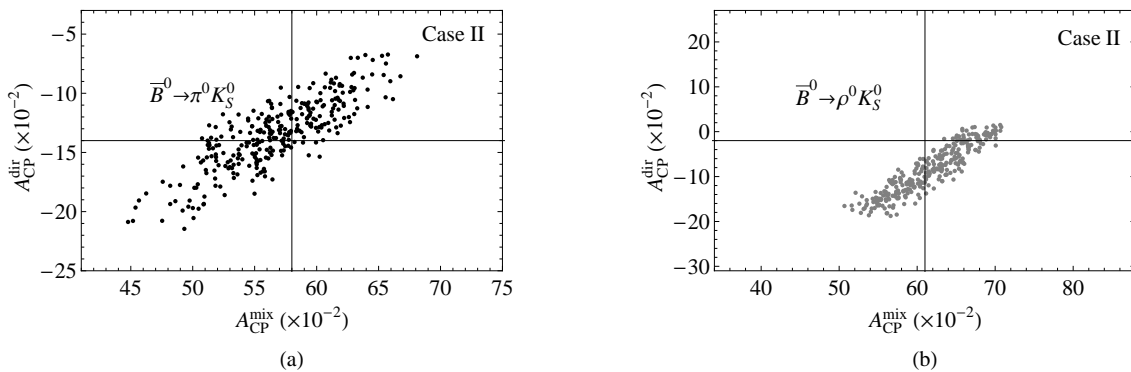


Figure 10: Correlation between direct and mixing-induced CP asymmetries for $\bar{B}^0 \rightarrow \pi^0 K_S$ (a) and $\bar{B}^0 \rightarrow \rho^0 K_S$ (b) in Case II with $m_g = 0.5 \text{ GeV}$. The lines are the central value of experimental data presented at ICHEP 08. Our plot ranges corresponding the experimental error-bars.

$\Delta S_{\rho^0 K_S} = -0.05 \pm 0.07$, which agree well with the results in the paper. Considering our different treatments of the end-piont divergences, the agreement numerically confirms the observation that the mixing induced CP violations are insensitive to strong phases in the decay amplitudes.

In summary, assuming NP effects entering $B \rightarrow \pi K, \pi K^*$ and ρK decays via $\bar{s}(S + P)b \otimes \bar{q}(S + P)q$ operators, we have performed fittings for the observables in these decays with a model-independent approach. It's found that all the experimental data, especially the direct CP violation difference ΔA , could be accommodated by new $b \rightarrow su\bar{u}$ or $b \rightarrow sd\bar{d}$ contributions, of course by their combination. Assuming the dominance of new $b \rightarrow su\bar{u}$ operators (Case I), we find the color-octet operator has the similar strength as the color-singlet one, which is rather exotic for electro-weak NP models. However, taking the new $b \rightarrow sd\bar{d}$ operators dominant (Cases II and III), we have shown that color-singlet operator $\bar{s}(S + P)b \otimes \bar{d}(S + P)d$ solely can provide a resolution to the derivations with a strength about half of $b \rightarrow su\bar{u}$ operators. We also have performed fits (Cases IV and V) with both $b \rightarrow su\bar{u}$ and $b \rightarrow sd\bar{d}$ contributions to infer their relative size in these decays. It is found that the strength of $b \rightarrow sd\bar{d}$ is stronger than that of $b \rightarrow su\bar{u}$. In all cases, to account for the experimental deviations from the SM predictions for direct CP violations, especially for $A_{CP}(B^- \rightarrow \pi^0 K^-)$, new electro-weak phase about 100° relative to the SM $b \rightarrow sq\bar{q}$ penguin amplitude is always required. With the fitted parameters, we present results for the mixing induced CP asymmetries in $\bar{B}^0 \rightarrow \pi^0 K_S$ and $\rho^0 K_S$ decays. It is found the NP effects generally reduce $S_{\pi^0 K_S}$ and $S_{\rho^0 K_S}$. However, due to the large error-bars, the present experimental data do not further reduce the parameter spaces of the NP operators.

4 Conclusions

At present, the successful running of the B factories with their detectors BABAR (SLAC) and BELLE (KEK) have already taken about 10^9 data together at $\Upsilon(4S)$ resonance, and have produced plenty of exciting results. Tensions between the experimental data and the SM predictions based on different approaches for strong dynamics are accumulated, which may be due to our limited understanding of the strong dynamics, but equally possible due to NP effects. Motivated by the recent observed ΔA of the difference in direct CP violation between $\mathcal{A}_{CP}(B^\mp \rightarrow \pi^0 K^\mp)$ and $A_{CP}(B^0 \rightarrow K^\pm \pi^\mp)$ and theoretical issues of endpoint divergences, strong phases and annihilation contributions in charmless hadronic B decays, we have revisited the $B \rightarrow \pi K, \pi K^*$ and ρK decays with an infrared finite form of the

gluon propagator supplemented to the QCDF approach. In this way, we can get large strong phases from the annihilation contributions, while the hard spectator-scattering amplitudes are real. From our numerical analyses, we find that the contributions of the annihilation and the hard-spectator topologies are sensitive to the value of the effective gluon mass m_g . With $m_g = 500 \pm 50$ MeV, our predictions in the SM agree with the current experimental data well, except $A_{CP}(B^\pm \rightarrow K^\pm \pi^0)$. Actually with m_g varying from 300 MeV to 700 MeV, we always get $\mathcal{A}_{CP}(B^\mp \rightarrow \pi^0 K^\mp) \approx A_{CP}(B^0 \rightarrow K^\pm \pi^\mp)$ as shown in Table 2, which also agree with the results in the literature. We conclude that NP effects is required, at least can not be excluded, to resolve the discrepancies between the observed ΔA and the SM expectations.

With four effective NP $b \rightarrow su\bar{u}$ and $b \rightarrow sdd\bar{d}$ operators, we have performed a model-independent approach to the discrepancies. Our main conclusions are summarized as:

- Assuming dominance of $b \rightarrow su\bar{u}$ operators, the fit gives a quite small center value for $A_{CP}(B^0 \rightarrow K^\pm \pi^\mp)$ although consistent with the data within its large error-bar. Moreover, the strength of color-octet operator O_{S8}^u is comparable with color-singlet O_{S1}^u which may be rather exotic for most NP models.
- With the $b \rightarrow sdd\bar{d}$ operator O_{S1}^d solely, the observables in $B \rightarrow \pi K, \pi K^*$ and ρK decays could be well accommodated, since $\bar{B}^0 \rightarrow K^- \pi^+$ is irrelevant to the $b \rightarrow sdd\bar{d}$ operator and it's branching ratio and CP violation agree with the SM prediction very well.
- Assuming dominance of color-singlet operators O_{S1}^u and O_{S1}^d , it is found that the two operators have the similar weak phase with $C_{S1}^u \approx \frac{1}{2}C_{S1}^d$.
- For all Cases, to account for the experimental deviations from the SM predictions for direct CP violations, especially for $A_{CP}(B^- \rightarrow \pi^0 K^-)$, new electro-weak phase about 100° relative to the SM $b \rightarrow sq\bar{q}$ penguin amplitude is always required.
- With the fitted parameter spaces, the NP operators decrease the mixing-induced CP violations in $B^0 \rightarrow \pi^0 K_S$ and $\rho^0 K_S$ decays, especially that of $\pi^0 K_S$ final states.

It is reminded that both direct and mixing-induced CP violations have not been well established in most of charmless nonleptonic B decays. Although the difference in direct CP asymmetries between $\mathcal{A}_{CP}(B^\mp \rightarrow \pi^0 K^\mp)$ and $A_{CP}(B^0 \rightarrow K^\pm \pi^\mp)$ shows some hints of new

physics activities, we still need refined measurements of the mixing-induced CP asymmetries in the related decays $B^0 \rightarrow \pi^0 K_S$ and $\rho^0 K_S$ to confirm or refute the NP hints, since the former strongly depends on strong phases in the decay amplitudes while the later not so much and can be predicted more precisely. In the coming years, the precision of experimental measurement of the observables in these decays will be improved much with LHCb at CERN, which will shrink the parameter space and reveal the relative importance of the five Cases studied in this paper. Then, the favored Case will deserve detail studies with particular NP models.

Acknowledgments

The work is supported by National Science Foundation under contract Nos.10675039 and 10735080. X.Q. Li acknowledges support from the Alexander-von-Humboldt Stiftung.

Appendix A: Decay amplitudes in the SM with QCDF

The amplitudes for $B \rightarrow \pi K$, πK^* and ρK are recapitulated from Ref. [3]

$$\mathcal{A}_{B^- \rightarrow \pi^- \bar{K}}^{\text{SM}} = \sum_{p=u,c} V_{pb} V_{ps}^* A_{\pi \bar{K}} \left[\delta_{pu} \beta_2 + \alpha_4^p - \frac{1}{2} \alpha_{4,\text{EW}}^p + \beta_3^p + \beta_{3,\text{EW}}^p \right], \quad (43)$$

$$\begin{aligned} \sqrt{2} \mathcal{A}_{B^- \rightarrow \pi^0 K^-}^{\text{SM}} &= \sum_{p=u,c} V_{pb} V_{ps}^* \left\{ A_{\pi^0 K^-} \left[\delta_{pu} (\alpha_1 + \beta_2) + \alpha_4^p + \alpha_{4,\text{EW}}^p + \beta_3^p + \beta_{3,\text{EW}}^p \right] \right. \\ &\quad \left. + A_{K^- \pi^0} \left[\delta_{pu} \alpha_2 + \frac{3}{2} \alpha_{3,\text{EW}}^p \right] \right\}, \end{aligned} \quad (44)$$

$$\mathcal{A}_{\bar{B}^0 \rightarrow \pi^+ K^-}^{\text{SM}} = \sum_{p=u,c} V_{pb} V_{ps}^* A_{\pi^+ K^-} \left[\delta_{pu} \alpha_1 + \alpha_4^p + \alpha_{4,\text{EW}}^p + \beta_3^p - \frac{1}{2} \beta_{3,\text{EW}}^p \right], \quad (45)$$

$$\begin{aligned} \sqrt{2} \mathcal{A}_{\bar{B}^0 \rightarrow \pi^0 \bar{K}^0}^{\text{SM}} &= \sum_{p=u,c} V_{pb} V_{ps}^* \left\{ A_{\pi^0 \bar{K}^0} \left[-\alpha_4^p + \frac{1}{2} \alpha_{4,\text{EW}}^p - \beta_3^p + \frac{1}{2} \beta_{3,\text{EW}}^p \right] \right. \\ &\quad \left. + A_{\bar{K}^0 \pi^0} \left[\delta_{pu} \alpha_2 + \frac{3}{2} \alpha_{3,\text{EW}}^p \right] \right\}, \end{aligned} \quad (46)$$

where the explicit expressions for the coefficients $\alpha_i^p \equiv \alpha_i^p(M_1 M_2)$ and $\beta_i^p \equiv \beta_i^p(M_1 M_2)$ can also be found in Ref. [3]. Note that expressions of the hard spectator terms H_i appearing in α_i^p and

the weak annihilation terms appearing in β_i^p should be replaced with our recalculated ones. The amplitudes of $B \rightarrow \pi K^*$ and $B \rightarrow \rho K$ decays could be obtained by setting $(\pi K) \rightarrow (\pi K^*)$ and $(\pi K) \rightarrow (\rho K)$, respectively.

Appendix B: Theoretical input parameters

B1. Wilson coefficients and CKM matrix elements

The Wilson coefficients $C_i(\mu)$ have been evaluated reliably to next-to-leading logarithmic order [24, 44]. Their numerical results in the naive dimensional regularization scheme at the scale $\mu = m_b$ ($\mu_h = \sqrt{\Lambda_h m_b}$) are given by

$$\begin{aligned} C_1 &= 1.074 (1.166), & C_2 &= -0.170 (-0.336), & C_3 &= 0.013 (0.025), \\ C_4 &= -0.033 (-0.057), & C_5 &= 0.008 (0.011), & C_6 &= -0.038 (-0.076), \\ C_7/\alpha_{e.m.} &= -0.016 (-0.037), & C_8/\alpha_{e.m.} &= 0.048 (0.095), & C_9/\alpha_{e.m.} &= -1.204 (-1.321), \\ C_{10}/\alpha_{e.m.} &= 0.204 (0.383), & C_{7\gamma} &= -0.297 (-0.360), & C_{8g} &= -0.143 (-0.168). \end{aligned} \quad (47)$$

The values at the scale μ_h , with $m_b = 4.80$ GeV and $\Lambda_h = 500$ MeV, should be used in the calculation of hard-spectator and weak annihilation contributions.

For the CKM matrix elements, we adopt the Wolfenstein parameterization [45] and choose the four parameters A , λ , ρ , and η as [46]

$$A = 0.807 \pm 0.018, \quad \lambda = 0.2265 \pm 0.0008, \quad \bar{\rho} = 0.141_{-0.017}^{+0.029}, \quad \bar{\eta} = 0.343 \pm 0.016, \quad (48)$$

with $\bar{\rho} = \rho(1 - \frac{\lambda^2}{2})$ and $\bar{\eta} = \eta(1 - \frac{\lambda^2}{2})$.

B2. Quark masses and lifetimes

As for the quark mass, there are two different classes appearing in our calculation. One type is the pole quark mass appearing in the evaluation of penguin loop corrections, and denoted by m_q . In this paper, we take

$$m_u = m_d = m_s = 0, \quad m_c = 1.64 \pm 0.09 \text{ GeV}, \quad m_b = 4.80 \pm 0.08 \text{ GeV}. \quad (49)$$

The other one is the current quark mass which appears in the factor r_χ^M through the equation of motion for quarks. This type of quark mass is scale dependent and denoted by \overline{m}_q . Here we take [47, 48]

$$\begin{aligned}\overline{m}_s(\mu)/\overline{m}_q(\mu) &= 27.4 \pm 0.4 [48], & \overline{m}_s(2 \text{ GeV}) &= 87 \pm 6 \text{ MeV} [48], \\ \overline{m}_b(\overline{m}_b) &= 4.20 \pm 0.07 \text{ GeV} [47],\end{aligned}\tag{50}$$

where $\overline{m}_q(\mu) = (\overline{m}_u + \overline{m}_d)(\mu)/2$, and the difference between u and d quark is not distinguished.

As for the lifetimes of B mesons, we take [47] $\tau_{B_u} = 1.638 \text{ ps}$ and $\tau_{B_d} = 1.530 \text{ ps}$ as our default input values.

B3. The decay constants and form factors

In this paper, we take the decay constants

$$\begin{aligned}f_B &= (216 \pm 22) \text{ MeV} [50], & f_{B_s} &= (259 \pm 32) \text{ MeV} [50], & f_\pi &= (130.7 \pm 0.4) \text{ MeV} [47], \\ f_K &= (159.8 \pm 1.5) \text{ MeV} [47] & f_{K^*} &= (217 \pm 5) \text{ MeV} [49], & f_\rho &= (209 \pm 2) \text{ MeV} [47].\end{aligned}\tag{51}$$

and the form factors [49]

$$\begin{aligned}F_0^{B \rightarrow \pi}(0) &= 0.258 \pm 0.031, & F_0^{B \rightarrow K}(0) &= 0.331 \pm 0.041, & V^{B \rightarrow K^*}(0) &= 0.411 \pm 0.033, \\ A_0^{B \rightarrow K^*}(0) &= 0.374 \pm 0.034, & A_1^{B \rightarrow K^*}(0) &= 0.292 \pm 0.028, & V^{B \rightarrow \rho}(0) &= 0.323 \pm 0.030, \\ A_0^{B \rightarrow \rho}(0) &= 0.303 \pm 0.029, & A_1^{B \rightarrow \rho}(0) &= 0.242 \pm 0.023.\end{aligned}\tag{52}$$

B4. The LCDAs of mesons and light-cone projector operators.

The light-cone projector operators of light pseudoscalar and vector meson in momentum space read [51, 3]

$$\begin{aligned}M_{\alpha\beta}^P &= \frac{if_P}{4} \left(\not{x} \gamma_5 \Phi_P(x) - \mu_P \gamma_5 \frac{k_2 \cdot k_1}{k_2 \cdot k_1} \phi_p(x) \right)_{\alpha\beta}, \\ (M_{\parallel}^V)_{\alpha\beta} &= -\frac{if_V}{4} \left(\not{x} \Phi_V(x) - \frac{m_V f_V^\perp}{f_V} \frac{k_2 \cdot k_1}{k_2 \cdot k_1} \phi_v(x) \right)_{\alpha\beta},\end{aligned}\tag{53}$$

where μ_P is defined as $m_b r_\chi^P/2$, and $f_P(V)$ is the decay constant. The chirally-enhanced factor appearing in this paper is defined as

$$\begin{aligned} r_\chi^\pi(\mu) &= \frac{2m_\pi^2}{m_b(\mu)2m_q(\mu)}, & r_\chi^K(\mu) &= \frac{2m_K^2}{m_b(\mu)(m_q + m_s)(\mu)}, \\ r_\chi^V(\mu) &= \frac{2m_V}{m_b(\mu)} \frac{f_V^\perp}{f_V}, \end{aligned} \quad (54)$$

where the quark masses are all running masses defined in the $\overline{\text{MS}}$ scheme which we have given in Appendix B2. For the LCDAs of mesons, we use their asymptotic forms [52, 53]

$$\Phi_P(x) = \Phi_V(x) = 6x(1-x), \quad \phi_p(x) = 1, \quad \phi_v(x) = 3(2x-1). \quad (55)$$

As for the B meson wave function, we take the form [54]

$$\Phi_B(\xi) = N_B \xi(1-\xi) \exp\left[-\left(\frac{M_B}{M_B - m_b}\right)^2 (\xi - \xi_B)^2\right], \quad (56)$$

where $\xi_B \equiv 1 - m_b/M_B$, and N_B is the normalization constant to make sure that $\int_0^1 d\xi \Phi_B(\xi) = 1$.

References

- [1] A. J. Buras, R. Fleischer, S. Recksiegel and F. Schwab, Phys. Rev. Lett. **92** (2004) 101804 [hep-ph/0312259]; Nucl. Phys. B **697** (2004) 133 [hep-ph/0402112]; PoS **HEP2005** (2006) 193 [hep-ph/0512059].
- [2] M. Beneke, G. Buchalla, M. Neubert, C. T. Sachrajda, Nucl. Phys. B **606** (2001) 245 [hep-ph/0104110]; M. Beneke and M. Neubert, Nucl. Phys. B **651** (2003) 225 [hep-ph/0210085].
- [3] M. Beneke and M. Neubert, Nucl. Phys. B **675** (2003) 333 [hep-ph/0308039].
- [4] T. Muta, A. Sugamoto, M. Z. Yang and Y. D. Yang, Phys. Rev. D **62** (2000) 094020 [hep-ph/0006022]; M. Z. Yang and Y. D. Yang, Phys. Rev. D **62** (2000) 114019 [hep-ph/0007038].
- [5] H. N. Li, S. Mishima and A. I. Sanda, Phys. Rev. D **72** (2005) 114005 [hep-ph/0508041].
- [6] A. R. Williamson and J. Zupan, Phys. Rev. D **74** (2006) 014003 [hep-ph/0601214].

- [7] M. Gronau and J. L. Rosner, Phys. Rev. D **74** (2006) 057503 [hep-ph/0608040]; X. Q. Li and Y. D. Yang, Phys. Rev. D **73** (2006) 114027 [hep-ph/0602224]; Phys. Rev. D **72** (2005) 074007 [hep-ph/0508079]; J. Chay, H. N. Li, arXiv: 0711.2953 [hep-ph]; C. W. Bauer, I. Z. Rothstein and I. W. Stewart, Phys. Rev. D **74** (2006) 034010 [hep-ph/0510241]; C. S. Kim, S. Oh, and C. Yu, Phys. Rev. D **72** (2005) 074005 [hep-ph/0505060];
- [8] S. Baek, JHEP **0607** (2006) 025 [hep-ph/0605094]; R. Arnowitt *et al.*, Phys. Lett. B **633** (2006) 748 [hep-ph/0509233]; S. Khalil, Phys. Rev. D **72** (2005) 035007 [hep-ph/0505151]; Y. D. Yang, R. M. Wang, G. R. Lu, Phys. Rev. D **73** (2006) 015003 [hep-ph/0509273]; V. Barger, C. W. Chiang, P. Langacker and H. S. Lee, Phys. Lett. B **598** (2004) 218 [hep-ph/0406126]; W. S.Hou, M. Nagashima and A. Soddu, Phys. Rev. Lett. **95** (2005) 141601 [hep-ph/0503072]; W. S.Hou, M. Nagashima, G. Raz and A. Soddu, JHEP **0609** (2006) 012 [hep-ph/0603097]; C. S. Kim, S. Oh and Y. W. Yoon, arXiv: 0707.2967 [hep-ph]; C. S. Kim, S. Oh, C. Sharma, R. Sinha and Y. W. Yoon Phys. Rev. D **76** (2007) 074019, arXiv: 0706.1150 [hep-ph].
- [9] S. W. Lin *et al.*, Belle Collaboration, Nature **452** (2008) 332.
- [10] B. Aubert *et al.*, Babar Collaboration, Phys. Rev. Lett. **99** (2007) 021603 [hep-ex/0703016].
- [11] S. Chen *et al.*, CLEO Collaboration, Phys. Rev. Lett. **85** (2000) 525 [hep-ex/0001009].
- [12] Michael Morello, CDF Collaboration, Nucl. Phys. Proc. Suppl. **170** (2007) 39 [hep-ex/0612018].
- [13] E. Barberio *et al.* (Heavy Flavor Averaging Group), arXiv: 0704.3575 [hep-ex]; and online update at: <http://www.slac.stanford.edu/xorg/hfag>.
- [14] M. Beneke, G. Buchalla, M. Neubert and C. T. Sachrajda, Phys. Rev. Lett. **83** (1999) 1914 [hep-ph/9905312]; Nucl. Phys. B **591** (2000) 313 [hep-ph/0006142].
- [15] Y. Y. Keum, H. N. Li and A. I. Sanda, Phys. Lett. B **504** (2001) 6 [hep-ph/0004004]; Phys. Rev. D **63** (2001) 054008 [hep-ph/0004173].
- [16] C. W. Bauer, S. Fleming and M. Luke, Phys. Rev. D **63** (2001) 014006 [hep-ph/0005275]; C. W. Bauer, S. Fleming, D. Pirjol and I. W. Stewart, Phys. Rev. D **63** (2001) 114020

- [hep-ph/0011336]; C. W. Bauer and I. W. Stewart, Phys. Lett. B **516** (2001) 134 [hep-ph/0107001]; C. W. Bauer, D. Pirjol and I. W. Stewart, Phys. Rev. D **65** (2001) 054022 [hep-ph/0109045].
- [17] M. E. Peskin, Nature **452** (2008) 293.
- [18] Th. Feldmann, M. Jung and Th. Mannel, arXiv: 0803.3729 [hep-ph].
- [19] Th. Feldmann and T. Hurth, JHEP **0411** (2004) 037 [hep-ph/0408188].
- [20] J. M. Cornwall, Phys. Rev. D **26** (1982) 1453; J. Papavassiliou and J. M. Cornwall, Phys. Rev. D **44** (1991) 1285.
- [21] A. C. Aguilar, A. A. Natale and P. S. Rodrigues da Silva, Phys. Rev. Lett. **90** (2003) 152001 [hep-ph/0212105]; A. C. Aguilar and A. A. Natale, JHEP **0408** (2004) 057 [hep-ph/0408254].
- [22] L. Von Smekal, A. Hauck, and R. Alkofer, Phys. Rev. Lett. **79** (1997) 3591 [hep-ph/9705242]; R. Alkofer and L. Von Smekal, Phys. Rep. **353** (2001) 281 [hep-ph/0007355]; C. S. Fisher and R. Alkofer, Phys. Rev. D **67** (2003) 094020 [hep-ph/0301094]; R. Alkofer, W. Detmold, C. S. Fisher, and P. Maris, Nucl. Phys. Proc. Suppl. **141** (2005) 122 [hep-ph/0309078].
- [23] I. L. Bogolubsky, E. -M. Ilgenfritz, M. Müller Preussker and A. Sternbeck, PoS (LATTICE-2007) 290, arXiv: 0710.1968 [hep-lat]; A. Cucchieri and T. Mendes, PoS (LATTICE 2007) 297, arXiv: 0710.0412 [hep-lat]; P. O. Bowman *et al.*, Phys. Rev. D **76** (2007) 094505, [hep-lat/0703022].
- [24] G. Buchalla, A. J. Buras, and M. E. Lautenbacher, Rev. Mod. Phys. **68** (1996) 1125 [hep-ph/9512380].
- [25] N. Cabibbo, Phys. Rev. Lett. **10** (1963) 531; M. Kobayashi and T. Maskawa, Prog. Theor. Phys. **49** (1973) 652.
- [26] D. S. Du, J. Korean Phys. Soc. **45** (2004) S285 [hep-ph/0311135]; D. S. Du, Int. J. Mod. Phys. A **21** (2006) 658 [hep-ph/0508287]; D. S. Du, J. F. Sun, D. S. Yang and G. H. Zhu,

- Phys. Rev. D **67** (2003) 014023 [hep-ph/0209233]; D. S. Du, H. J. Gong, J. F. Sun, D. S. Yang and G. H. Zhu, Phys. Rev. D **65** (2002) 094025 [hep-ph/0201253]; D. S. Du, D. S. Yang and G. H. Zhu, Phys. Rev. D **64** (2001) 014036 [hep-ph/0103211]; Phys. Lett. B **509** (2001) 263 [hep-ph/0102077]; Phys. Lett. B **488** (2000) 46 [hep-ph/0005006].
- [27] D. Zwanziger, Phys. Rev. D **69** (2004) 016002 [hep-ph/0303028]; D. M. Howe and C. J. Maxwell, Phys. Lett. B **541** (2002) 129 [hep-ph/0204036]; Phys. Rev. D **70** (2004) 014002 [hep-ph/0303163]; S. Furui and H. Nakajima, AIP Conf. Proc. **717**, (2004) 685 [hep-lat/0309166].
- [28] S. Brodsky, S. Menke, C. Merino and J. Rathsman, Phys. Rev. D **67** (2003) 055008 [hep-ph/0212078]; A. C. Mattingly and P. M. Stevenson, Phys. Rev. D **49** (1994) 437 [hep-ph/9307266]; M. Baldicchi, G. M. Prosperi, Phys. Rev. D **66** (2002) 074008 [hep-ph/0202172].
- [29] F. Su, Y. D. Yang, G. R. Lu and H. J. Hao, Eur. Phys. J. C **44** (2005) 243 [hep-ph/0507326]; F. Su, Y. L. Wu, Y. D. Yang and C. Zhuang, Eur. Phys. J. C **48** (2006) 401 [hep-ph/0604082]; arXiv: 0705.1575 [hep-ph].
- [30] A. A. Natale and C. M. Zanetti, arXiv: 0803.0154 [hep-ph].
- [31] S. Baek, A. Datta, P. Hamel, O. F. Hernandez and D. London, Phys. Rev. D **72** (2005) 094008 [hep-ph/0508149]; S. Baek and D. London, Phys. Lett. B **653** (2007) 249 [hep-ph/0701181].
- [32] W. S. Hou, M. Nagashima and A. Suddu, Phys. Rev. Lett. **95** (2005) 141601 [hep-ph/0503072].
- [33] A. L. Kagan, Phys. Lett. B **601** (2004) 151 [hep-ph/0405134].
- [34] P. K. Das and K. C. Yang, Phys. Rev. D **71** (2005) 094002 [hep-ph/0412313].
- [35] H. Hatanaka and K. C. Yang, Phys. Rev. D **77** (2008) 035013, arXiv: 0711.3086 [hep-ph].
- [36] Q. Chang, X. Q. Li and Y. D. Yang, JHEP **0706** (2007) 038 [hep-ph/0610280].
- [37] S. Nandi and A. Kundu, J. Phys. G **32** (2006) 835 [hep-ph/0510245].

- [38] M. Beneke, Phys. Lett. B **620** (2005) 143 [hep-ph/0505075].
- [39] G. Buchalla, G. Hiller, Y. Nir and G. Raz, JHEP **0509** (2005) 074 [hep-ph/0503151].
- [40] R. Fleischer, S. Jager, D. Pirjol and J. Zupan, arXiv: 0806.2900 [hep-ph].
- [41] M. Gronau and J. Rosner, arXiv:0807.3080[hep-ph].
- [42] James F. Hirschauer (BABAR Collaboration), talk presented at ICHEP08, the 34th International Conference on High Energy Physics Philadelphia, Pennsylvania, July 30 - August 5, 2008.
- [43] Jeremy P Dalseno (Belle Collaboration), talk presented ICHEP08.
- [44] A. J. Buras, P. Gambino, and U. A. Haisch, Nucl. Phys. B **570** (2000) 117 [hep-ph/9911250].
- [45] L. Wolfenstein, Phys. Rev. Lett. **51** (1983) 1945.
- [46] J. Charles *et al.* (CKMfitter Group), Eur. Phys. J. C **41** (2005) 1 [hep-ph/0406184]; updated results and plots available at: <http://ckmfitter.in2p3.fr>.
- [47] W.M. Yao *et al.* (Particle Data Group), J. Phys. G **33** (2006) 1.
- [48] Q. Mason *et al.* (HPQCD Collaboration), Phys. Rev. D **73** (2006) 114501 [hep-ph/0511160].
- [49] P. Ball and R. Zwicky, Phys. Rev. D **71** (2005) 014015 [hep-ph/0406232]; **71** (2005) 014029 [hep-ph/0412079]; Phys. Lett. B **633** (2006) 289 [hep-ph/0510338].
- [50] A. Gray *et al.* (HPQCD Collaboration), Phys. Rev. Lett. **95** (2005) 212001 [hep-lat/0507015].
- [51] B. V. Geshkenbein and M. V. Terentev, Yad. Fiz. **40** (1984) 758; Sov. J. Nucl. Phys. **40** (1984) 487.
- [52] M. Beneke and Th. Feldmann, Nucl. Phys. B **592** (2001) 3 [hep-ph/0008255].

- [53] A. Ali *et al.*, Phys. Rev. D **61** (2000) 074024 [hep-ph/9910221]; P. Ball and V. M. Braun, Phys. Rev. D **58** (1998) 094016 [hep-ph/9805422]; P. Ball *et al.*, Nucl. Phys. B **529** (1998) 323 [hep-ph/9802299].
- [54] G. Eilam, M. Ladisa and Y. D. Yang, Phys. Rev. D **65** (2002) 037504 [hep-ph/0107043].